GEORGIA INSTITUTE OF TECHNOLOGY
School of Mechanical Engineering
Atlanta, Georgia

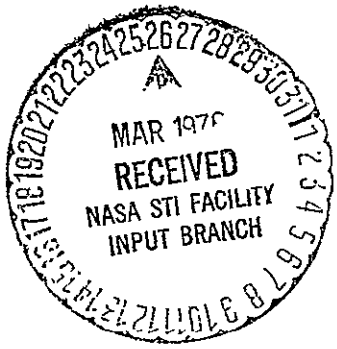

PREDICTION OF CRYOGENIC HEAT PIPE PERFORMANCE

ANNUAL REPORT FOR 1975

REPORT NUMBER II

Prepared for the
National Aeronautics and Space Administration
Under
Grant NSG-2054

Prepared by

Gene T. Colwell, Associate Professor
School of Mechanical Engineering
Georgia Institute of Technology
Atlanta, Georgia 30332

February 1, 1976

PREDICTION OF CRYOGENIC HEAT PIPE PERFORMANCE
ANNUAL REPORT FOR 1975
REPORT NUMBER II

Prepared for the

National Aeronautics and Space Administration
Under
Grant NSG-2054

Prepared by

Gene T. Colwell, Associate Professor
School of Mechanical Engineering
Georgia Institute of Technology
Atlanta, Georgia 30332

February 1, 1976

GEORGIA INSTITUTE OF TECHNOLOGY
School of Mechanical Engineering
Atlanta, Georgia 30332

NASA Grant NSG-2054

Annual Report for 1975

Report Number II

February 1, 1976

Approved:

S. P. Kezios, Director
School of Mechanical Engineering

G. T. Colwell
Principal Investigator

W. M. Sangster
Dean of Engineering

D. L. Allen, Deputy Director
Office of Contract Administration

CONTENTS

ACKNOWLEDGEMENTS

The writer wishes to acknowledge the essential contributions to this program made by people associated with NASA and Georgia Tech. At Georgia Tech James Hare, Don Priester, and David Ruis handled programing and operation of the digital and analog computers used to generate the data presented herein. Jack Kirkpatrick, Bob Debs, Manfred Groll, Craig McCreight, and Masahide Murakami of the NASA Ames Research Center reviewed the work at various stages and made valuable suggestions. Stan Ollendorf of the NASA Goddard Space Flight Center was primarily responsible for initiation of the project and he has continually provided encouragement, supervision and direction. Allan Sherman, of GSFC, has worked closely with the GIT team for about two years. He has suggested sizes, shapes, temperature ranges, and heat fluxes of current practical interest. In addition he has offered constructive criticism of the theoretical approaches used. The writer also wishes to acknowledge the contributions of Yashu Kamotani and Roy McIntosh of GSFC, who reviewed the theoretical approaches.

LIST OF FIGURES

LIST OF FIGURES CON'T

LIST OF TABLES

INTRODUCTION

In January of 1975 work was started at Georgia Tech on a project aimed at gaining a better understanding of the various design parameters which affect steady state and transient operation of cryogenic heat pipes. This report briefly describes the progress made on the project during the period January through December of 1975. Financial support has come from NASA under grant NSG-2054 and the work has been monitored by Jack Kirkpatrick of Ames Research Center and Stan Ollendorf of Goddard Space Flight Center. One M.S. thesis (reference 1) which is directly related to the project was published in June of 1975 and a second thesis in the area is currently being prepared and should be published about July 1976. It is anticipated that several papers will be published in recognized technical journals over the next few years as a result of the work.

Heat Pipe Under Study

A 304 stainless steel heat pipe with slab type capillary structure and nitrogen as the working fluid was studied in the temperature range of 60°K to 120°K. The pipe is 1.27 cm in outside diameter and 9.14 cm in total length. Figures 1 and 2 show geometry of the pipe and the configuration of the capillary structure. In the transient studies, described in detail in this report, saddles are included at evaporator and condenser ends and a radiator is included at the condenser end.

Summary of Results to Date

The work performed under the grant is divided into two main areas. The first area includes development of accurate steady state equations for predicting capillary limitations and development of equations for

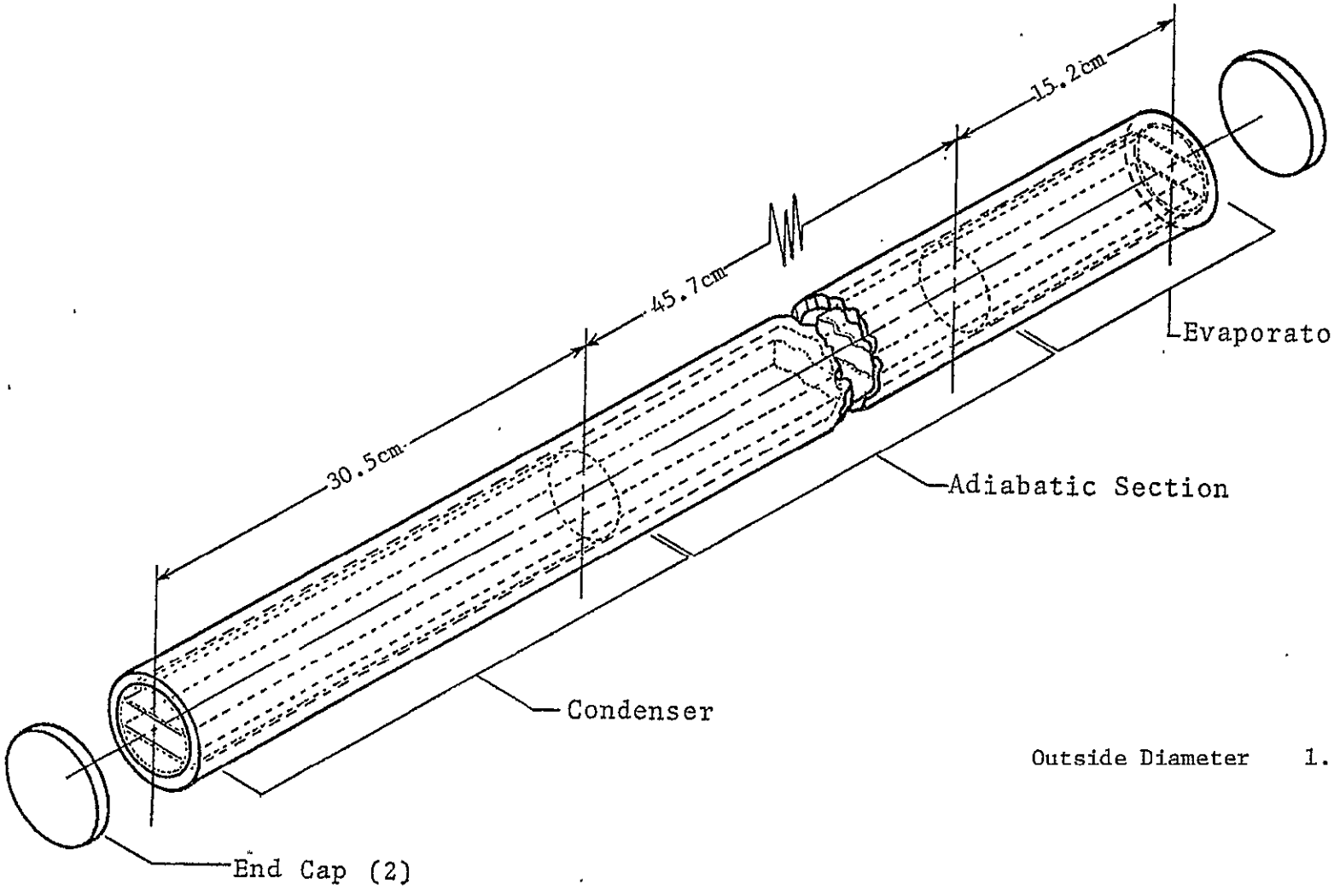

Outside Diameter 1.27 cm

Figure 1. General Layout of Heat Pipe

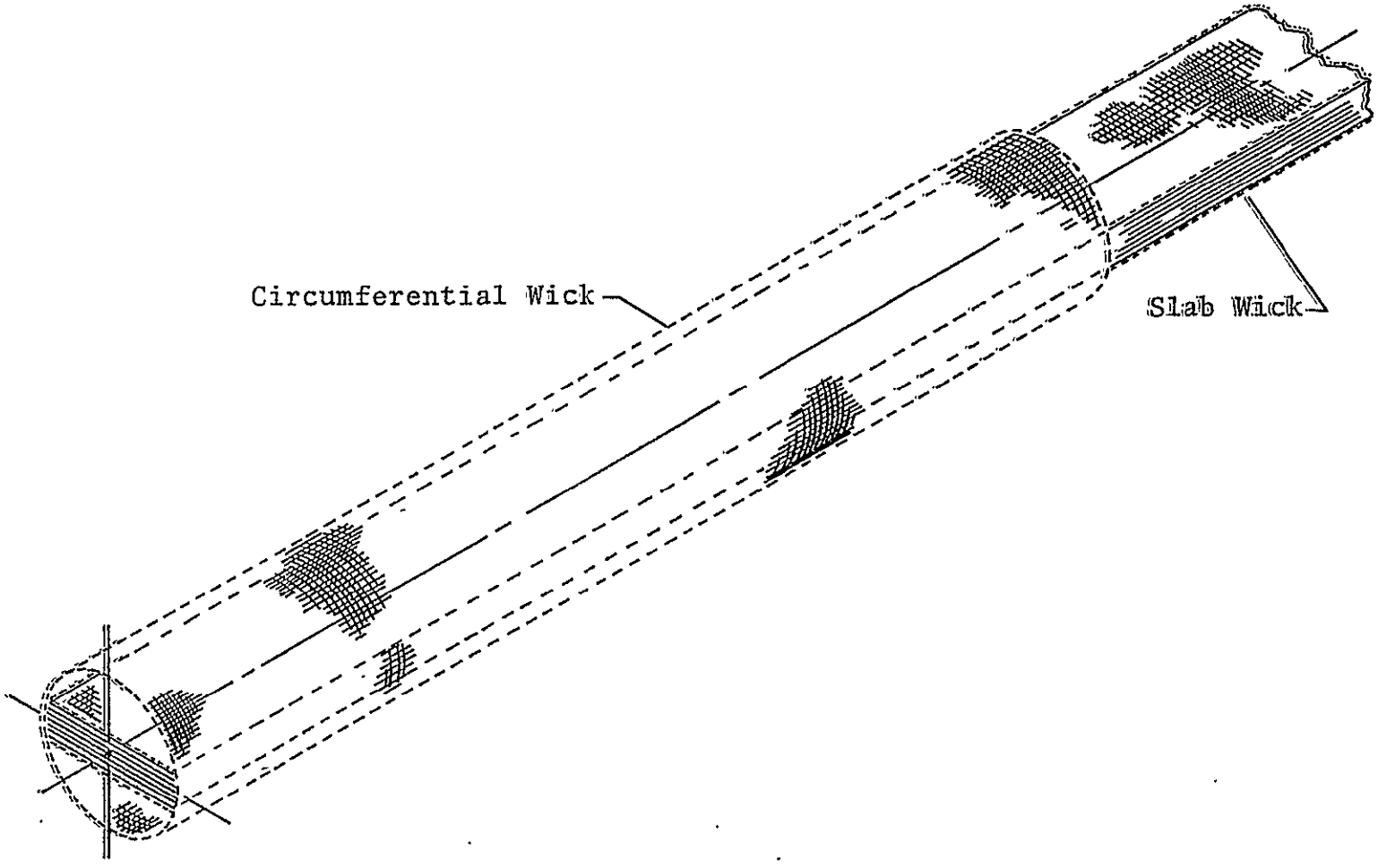

Figure 2. Close-Up of Composite Slab and Circumferential Wick at Heat Transfer Section

predicting thermal resistances. Extensive computer surveys were run using the equations developed and it was found that a heat pipe of the type described above could transfer as much as 30 to 40 watts with an overall temperature drop of a few degrees Kelvin. The second area of study was the transient operation of cryogenic heat pipes. The problem was first studied with the aid of an analog computer and currently a digital computer approach is being pursued. Results of the analog work, which is limited to small transients and does not account for fluid dynamics, show the effects of small step temperature changes and the effects of fast and slow sine wave variations of small amplitude on heat pipe operating parameters. The digital program now under development will be much more powerful in that large transients, even including the case of start-up from the supercritical state, can be studied. At present a simplified model, which does not include fluid dynamic effects, is being successfully examined on a digital computer. The next step is to incorporate fluid dynamic effects.

Future Plans

The main theoretical effort is now being directed towards making the transient model, which is being examined on a digital computer, more realistic and more flexible. It is expected that this work will require another six months assuming that current levels of effort are maintained.

Some effort is now being directed to planning some low temperature heat pipe experiments which could be used to generate data for verifying and modifying both steady state and transient models. In the near term the experiments would be carried out in a laboratory on earth. Also some initial thought has been given to the idea of a space experiment. The National Aeronautics and Space Administration currently is designing

a "Long Duration Exposure Facility" and a "Sky Lab" either of which would be ideal for this type of space experiment.

RESULTS TO DATE

During Calendar 1975 significant progress has been made both in the steady state and transient parts of the work. Computer programs are now on hand for predicting capillary limitations, and steady state thermal resistances for slab type cryogenic heat pipes. An analog scheme has been developed which handles small transients and work is progressing on a much more powerful digital solution scheme which will be able to handle large transients including startup from the supercritical region. Each of these steady state and transient approaches will be discussed in detail.

Steady State Thermal Resistances

In the typical design of a heat pipe, little attention is given to predicting thermal resistances. This is the case because accurate predictions are extremely difficult in most systems. It is not uncommon to underestimate overall heat pipe temperature drops by an order of magnitude.

In the present analysis resistances are considered in the pipe wall at the condenser and evaporator, in the layers of capillary material around the circumference of the evaporator and condenser surfaces, in the fluid gaps between layers of capillary material, at liquid vapor interfaces, and in the vapor region. In addition it has been assumed that the circumferential portion of the capillary structure partially drys as heat transfer is increased towards the capillary limitation. This problem is discussed in detail in references 2 through 5. Results of several studies, see reference 2, suggest that in long heat pipes part of the condenser surface may not be active at relatively low heat

transfer rates. This effect has been considered in developing a thermal resistance model at the condenser end.

The following nomenclature is used in computing thermal resistances.

d_f distance between centers of screen filaments

g_c conversion factor

h_{fg} enthalpy of vaporization of N_2

k_f conductivity of stainless steel screen filaments or of the stainless steel pipe

k_ℓ conductivity of liquid nitrogen

k_p conductivity of stainless steel pipe

k_w conductivity of the liquid filled screen portion of the wick

ℓ_{ax} axial length

ℓ_{ca} active condenser length

ℓ_{cd} length of condenser at design conditions

ℓ_E length of evaporator section

ℓ_{eff} effective length of vapor path

N number of screen layers

p_v vapor pressure

Q heat transfer rate

Q_{MAX} capillary limitation

R ideal gas constant

r_A outer radius of pipe wall

r_B inner radius of pipe wall

r_C inner radius of wick

r_{CHD} hydraulic radius of complete wick structure

r_f distance between centers of screen filaments

R_{IC} resistance of interface at condenser

R_{IE} resistance of liquid vapor interface at evaporator

R_{PC} resistance of pipe wall at condenser

R_{PE} resistance of pipe wall at evaporator

R_{TOT} total resistance

R_V resistance of vapor

R_{WC} resistance of wick at condenser

R_{WE} resistance of wick at evaporator

T_C temperature of outer surface of pipe at condenser

T_E temperature of outer surface of pipe at evaporator

T_{LI} temperature of liquid at the liquid vapor interface

T_{PCI} temperature of inner surface of pipe at condenser

T_{PEI} temperature of inner surface of pipe at evaporator

T_V vapor temperature

W_T wall thickness of pipe

β thickness of liquid layers between screen layers

ΔT $T_E - T_C$

μ_v viscosity of vapor

ρ_ℓ density of liquid

ρ_v density of vapor

θ angle within each quadrant over which liquid is present in the wick at the evaporator

δ_T thickness of central slab

The equations developed for computing resistances are given in the following list.

The resistance of circumferential layers of capillary structure and working fluid gaps is (see Figure 3)

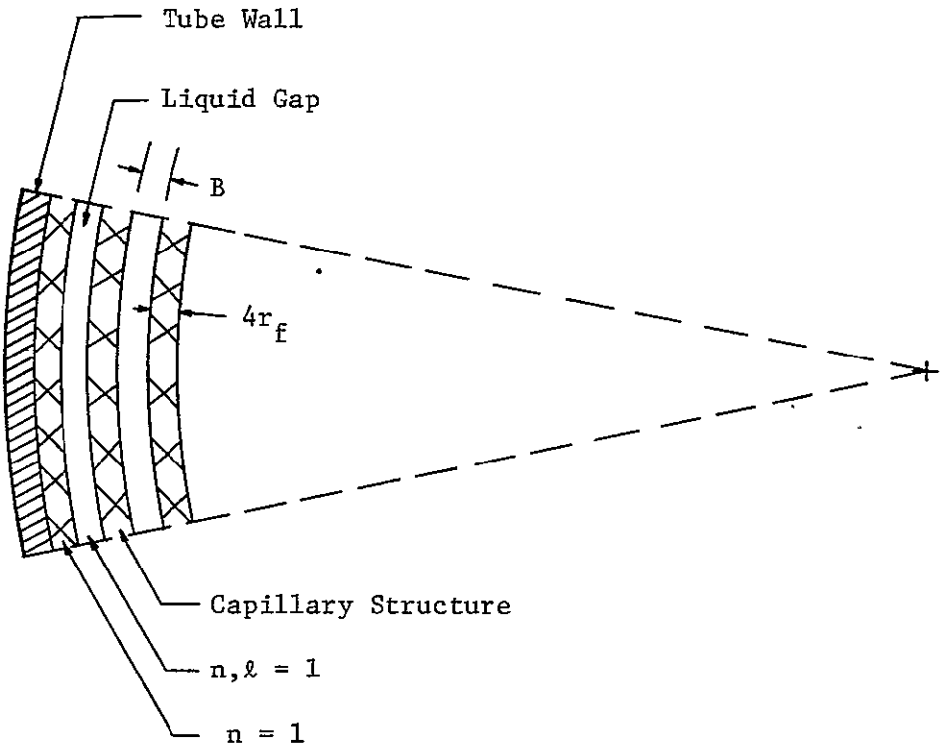

Figure 3. Capillary Structure

$$R_w = \sum_{n=1}^{N} R_n + \sum_{n=1}^{N-1} R_{n,\ell} \tag{1}$$

$$R_n = \frac{\ell n \dfrac{r_B - (n-1)4r_f - (n-1)\beta}{r_B - n4r_f - (n-1)\beta}}{2\pi\, k_w\, \ell_{ax}} \tag{2}$$

$$R_{n,\ell} = \frac{\ell n \dfrac{r_B - n4r_f - (n-1)\beta}{r_B - n4r_f - n\beta}}{2\pi\, k_\ell\, \ell_{ax}} \tag{3}$$

Dry out of the evaporator surface is accounted for by (see Figure 4)

$$\theta = \frac{\frac{\pi}{2}}{1 + \frac{Q}{Q_{MAX}}} \tag{4}$$

Assume that the active condenser length is $\ell_{ca} = \ell_{cd} \dfrac{Q}{Q_{MAX}}$.

The wick resistance at the condenser then becomes

$$R_{WC} = \sum_{n=1}^{N} R_n + \sum_{n=1}^{N-1} R_{n,\ell} \tag{5}$$

$$R_n = \frac{\dfrac{Q_{MAX}}{Q}\ \ell n \dfrac{r_B - (n-1)4r_f - (n-1)\beta}{r_B - 4nr_f - (n-1)\beta}}{2\pi\, k_w\, \ell_{cd}} \tag{6}$$

$$R_{n\ell} = \frac{\dfrac{Q_{MAX}}{Q}\ \ell n \dfrac{r_B - 4nr_f - (n-1)\beta}{r_B - 4nr_f - n\beta}}{2\pi\, k_\ell\, \ell_{cd}} \tag{7}$$

The wick resistance at the evaporator is

$$R_{WE} = \left[1 + \frac{Q}{Q_{MAX}}\right] \left[\sum_{n=1}^{N} R_n + \sum_{n=1}^{N-1} R_{n,\ell}\right] \tag{8}$$

$$R_n = \frac{\ell n \dfrac{r_B - (n-1)\ 4r_f - (n-1)\beta}{r_B - 4n\ r_f - (n-1)\beta}}{2\pi\ k_w\ \ell_E} \tag{9}$$

$$R_{n,\ell} = \frac{\ell n \dfrac{r_B - 4nr_f - (n-1)\beta}{r_B - 4nr_f - n\beta}}{2\pi\ k_\ell\ \ell_E} \tag{10}$$

The effective thermal conductivity of the fluid-metal combination in a typical single layer is (reference 2)

$$k_w = k_\ell \left\{ \frac{1}{\dfrac{d_f}{2r_f}\left[2\,\dfrac{k_\ell}{k_f} + \dfrac{d_f}{2r_f} - 2\right]} + \frac{2}{\dfrac{d_f}{2r_f}\left(\dfrac{k_\ell}{k_f}\right)\left[\dfrac{2r_f}{d_f - 2r_f} + 1\right]} + \frac{1}{\left[\dfrac{2r_f}{d_f - 2r_f} + 1\right]^2} \right\} \tag{11}$$

The resistance of the pipe wall in the condenser and evaporator sections is

$$R_{PC} = \frac{Q_{MAX}}{Q}\ \frac{\ell n \dfrac{r_A}{r_B}}{2\pi\ k_f\ \ell_{cd}} \tag{12}$$

$$R_{PE} = \left[1 + \frac{Q}{Q_{MAX}}\right] \frac{\ell n \dfrac{r_A}{r_B}}{2\pi\ k_f\ \ell_E} \tag{13}$$

The interfacial resistances at condenser and evaporator ends is approximated as

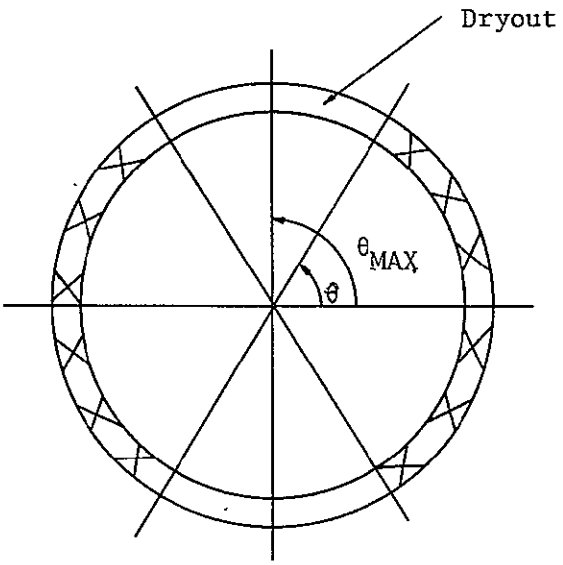

Figure 4. Dryout Angles

$$R_{IC} = \frac{Q_{MAX}}{Q} \frac{(2\pi)^{1/2} R^{3/2} T_{LI}^{5/2}}{4\pi r_c \ell_{cd} p_v h_{fg}^2 g_c^{1/2}} \tag{14}$$

$$R_{IE} = \left[1 + \frac{Q}{Q_{MAX}}\right] \frac{(2\pi)^{1/2} R^{3/2} T_{LI}^{5/2}}{4\pi r_c \ell_E p_v h_{fg}^2 g_c^{1/2}} \tag{15}$$

The resistance of the vapor is computed by assuming fully developed laminar flow and accounting for the obstruction presented by the slab with a hydraulic diameter.

$$R_V = \frac{8 \mu_v \ell_{eff} T_V \left(\frac{1}{p_v} - \frac{1}{\rho_\ell}\right)}{\pi \rho_v h_{fg}^2 r_{CHD}} \tag{16}$$

$$r_{CHD} = \frac{\pi r_C^2 - 2 r_C \delta_T}{2\pi r_C - 2 \delta_T + 4 r_C} \tag{17}$$

Hare (reference 1) has developed equations, based on National Bureau of Standards data, which give nitrogen properties and stainless steel properties in the temperature range of 60°K to 125°K.

Vapor Pressure $[lb_f/ft^2]$

$$p_v = 1.71041 \times 10^{-6} (T)^5 - 1.20901 \times 10^{-3} (T)^4 + 3.71275 \times 10^{-1} (T)^3 - 5.70868 \times 10(T)^2 + 4.28513 \times 10^3 (T) - 1.25125 \times 10^5 \tag{18}$$

Density of Liquid and Vapor $[lb_m/ft^3]$

$$\rho_\ell = - 5.8917 \times 10^{-13} (T)^7 + 4.50297 \times 10^{-10} (T)^6 - 1.15298 \times 10^{-7} (T)^5 + 4.95327 \times 10^{-6} (T)^4 + 2.9749 \times 10^{-3} (T)^3 - 5.98552 \times 10^{-1} (T)^2 + 4.54425 \times 10 (T) - 1.21455 \times 10^3 \tag{19}$$

$$\rho_v = 1.39324 \times 10^{-13} (T)^7 - 1.042325 \times 10^{-10} (T)^6 + 2.638736 \times 10^{-8} (T)^5 - 1.14015 \times 10^{-6} (T)^4 - 6.78395 \times 10^{-4} (T)^3 + 1.385389 \times 10^{-1} (T)^2 - 1.07628 \times 10 (T) + 3.10045 \times 10^2 \quad (20)$$

Viscosity of Vapor and Liquid $[(lb_f - sec)/ft^2]$

$$\mu_v = 8.55910 \times 10^{-21} (T)^7 - 6.55918 \times 10^{-18} (T)^6 + 1.70105 \times 10^{-15} (T)^5 - 8.08553 \times 10^{-14} (T)^4 - 4.27309 \times 10^{-11} (T)^3 + 8.90377 \times 10^{-9} (T)^2 - 6.94007 \times 10^{-7} (T) + 1.99577 \times 10^{-5} \quad (21)$$

$$\mu_\ell = 4.48282 \times 10^{-14} (T)^4 + 2.34251 \times 10^{-11} (T)^3 - 3.55312 \times 10^{-9} (T)^2 + 3.14221 \times 10^{-8} (T) + 2.16226 \times 10^{-5} \quad (22)$$

Thermal Conductivity of Liquid Nitrogen $\left[\frac{Btu}{hr\ ft\ ^\circ R}\right]$

$$k_\ell = 1.0970566 \times 10^{-11} (T)^5 - 9.2427627 \times 10^{-9} (T)^4 + 3.090593 \times 10^{-6} (T)^3 - 5.1457532 \times 10^{-4} (T)^2 + 4.2210737 \times 10^{-2} (T) - 1.26105 \quad (23)$$

Heat of Vaporization $[Btu/lb_m]$

$$h_{fg} = - 4.11334 \times 10^{-11} (T)^6 + 2.0908 \times 10^{-8} (T)^5 - 1.43119 \times 10^{-6} (T)^4 - 1.03235 \times 10^{-3} (T)^3 + 2.61594 \times 10^{-1} (T)^2 - 2.40246 \times 10 (T) + 8.89614 \times 10^2 \quad (24)$$

Surface Tension $[lb_f/ft]$

$$\sigma = 6.70239 \times 10^{-12} (T)^4 - 4.60497 \times 10^{-9} (T)^3 + 1.19096 \times 10^{-6} (T)^2 - 1.44813 \times 10^{-4} (T) + 7.58324 \times 10^{-3} \quad (25)$$

Ratio of Specific Heats of Nitrogen

$$k = 1.572403 \times 10^{-6} (T)^2 - 8.6844907 \times 10^{-4} (T) + 1.52913275 \quad (26)$$

Thermal Conductivity of Stainless Steel [Btu/ft hr °R]

$$k_f = - 4.02016 \times 10^{-5} (T)^2 + 3.20878 \times 10^{-2} (T) + 1.30266 \quad (27)$$

where T = temperature in degrees Rankine.

For any heat pipe of specific structure there are four primary variables directly related to the thermal properties of the heat pipe. These are T_E, T_C, T_V, and Q. Among these four variables any two are independent while the other two are dependent.

The present numerical procedure involves first specifying Q and T_C and then making use of the fundamental relationship of temperature, resistance, and heat transfer rate to calculate temperatures at several locations along the path of heat flow and to calculate the thermal resistance of the various sections of the heat pipe. The temperatures calculated are only approximate since the simple resistance equation

$$Q = \frac{\Delta T}{R}$$

is based on the assumption of constant conductivity across the heat flow path between the two locations at which the temperatures are known. This approximation should not lead to appreciable errors since the length of each heat flow path considered is small and consequently the value of ΔT is small.

The equations which results from applying this method cannot be solved analytically because of the presence of high order terms, so an iterative solution is necessary. The iteration process used in this analysis converges rapidly on the solution, partly as a result of knowing the range in which the solution lies, so that the computer time required for this portion of the numerical analysis is not large. The iterative procedure converged on the solution to an accuracy of 4 decimal places in an average of only 2 iterations.

An outline of the numerical procedure is now given

I. Specify Q and T_C

(Q will vary from 10 Watts to 30 Watts)

(T_C will range from 60°K to 125°K)

Approximation: $T_{LI} \cong T_V$

This is an excellent approximation since the resistance of the liquid-vapor interface is extremely small. (R_I is typically about 0.0001 °K/Watt)

The properties of each section will be evaluated at a temperature which is the mean of the temperature of the boundaries of the section.

Algebraic manipulation of the equation $Q = (T_{PCI} - T_C)/R_{PC}$ yields

$$\frac{\alpha_1}{4} T_{PCI}^3 + \left(\frac{\alpha_1 T_C}{2} + \frac{\alpha_2}{2} - \frac{\alpha_1 T_C}{4} \right) T_{PCI}^2 + \left(\frac{\alpha_1 T_C^2}{4} + \frac{\alpha_2 T_C}{2} + \alpha_3 - \frac{\alpha_1 T_C^2}{2} - \frac{T_C \alpha_2}{2} \right) T_{PCI}$$

$$+ \left(- \frac{\alpha_1}{4} T_C^3 - \frac{\alpha_2}{2} T_C^2 - \alpha_3 T_C - \frac{Q_{MX}}{2\pi \ell_{cd}} \ell n \frac{r_A}{r_B} \right) = 0 \qquad (28)$$

where $\alpha_1 = -4.02016 \times 10^{-5}$ $\alpha_2 = 3.20878 \times 10^{-2}$ $\alpha_3 = 1.30266$

II. Solve equation 28 for T_{PCI}.

III. Assume a value for T_V and compute $T' = (T_V + T_{PCI})/2$.

IV. Compute k_ℓ from equation 23 for $T = T'$.

V. Compute k_f from equation 27 for $T = T'$.

VI. Compute k_w from equation 11.

VII. Compute $\sum_{n=1}^{N} R_n$ from equation 6.

VIII. Compute $\sum_{n=1}^{N-1} R_{n,\ell}$ from equation 7.

IX. Solve Equation 29 for T_V using linear interpolation method, repeating steps IV, V, AND VI.

$$\frac{T_V - T_{PCI}}{Q\sum_{n=1}^{N} R_n + Q\sum_{n=1}^{N-1} R_{n,\ell}} - 1 = 0 \qquad (29)$$

X. Compute R_{WC} from equation 5.

XI. Take $T' = \left[T_{PEI} + T_V\right] / 2$.

XII. Compute k_ℓ from equation 23 at T'.

XIII. Compute k_f from equation 27 at T'.

XIV. Compute k_w from equation 11 at T'.

XV. Assume values of T_{PEI} and determine T_{PEI} using iteration, repeating steps XI through XIV and using equation 30.

$$\frac{T_{PEI} - T_V}{Q\left[1 + \frac{Q}{Q_{MAX}}\right]\left\{\sum_{n=1}^{N} R_n + \sum_{n=1}^{N-1} R_{n,\ell}\right\}} - 1 = 0 \qquad (30)$$

XVI. Compute R_{WE} from equation 8.

XVII. Solve equation 31 for T_E.

Substituting metal conductivity equation into $Q = (T_E - T_{PEI})/R_{PE}$ gives

$$\frac{\alpha_1}{4} T_E^3 + \left(-\frac{\alpha_1}{4} T_{PEI} + \frac{\alpha_1}{2} T_{PEI} + \frac{\alpha_2}{2} \right) T_E^2$$

$$+ \left(-\frac{\alpha_1}{2} T_{PEI}^2 - \frac{\alpha_2}{2} T_{PEI} + \frac{\alpha_1}{4} T_{PEI}^2 + \frac{\alpha_2}{2} T_{PEI} + \alpha_3 \right) T_E \qquad (31)$$

$$+ \left(-\frac{\alpha_1}{4} T_{PEI}^3 - \frac{\alpha_2}{2} T_{PEI}^2 - \alpha_3 T_{PEI} - \frac{Q \ln \frac{r_A}{r_B}}{4\theta \ell_E} \right) = 0$$

XVIII. Compute k_{pE} from equation 27.

XIX. Compute R_{PE} from equation 13.

XX. Compute h_{fg} from equation 24 at $T = T_V$

XXI. Compute p_v from equation 18 at $T = T_V$

XXII. Compute R_{IC} from equation 14 at $T = T_V$

XXIII. Compute R_{IE} from equation 15.

XXIV. Let $\ell_{eff} = 3.0 \text{ ft} - \ell_E/2 - \left(\ell_{cd}/2\right)Q/Q_{MAX}$

XXV. Compute μ_v from equation 21.

XXVI. Compute ρ_v from equation 18.

XXVII. Compute ρ_ℓ from equation 19.

XXVIII. Compute R_V from equation 16.

XXIX. Compute $R_{TOT} = R_{PE} + R_{WE} + R_{IE} + R_V + R_{IC} + R_{WC} + R_{PC}$ and alternate equation $R_{TOT} = \left(T_E - T_C\right)/Q$.

The complete computer program is given in Appendix A.

The effects on thermal resistance of changing the size of liquid gaps, wall thickness, mesh size, and number of circumferential layers of capillary structure has been examined on the computer for a nitrogen heat pipe. Table I shows some of the geometries studied. Figures 5 through 21 show how temperature difference and resistance change with changes in operating temperature and heat flux for the cases described in Table I.

Several figures related to Cases 1 and 6 are included to show order of magnitudes for resistances for these two extreme cases. Only one plot is given for each of the other cases. It is interesting to note that overall temperature difference may increase or decrease with increasing vapor temperature at constant heat flux. For example in Case 1 the heat pipe temperature difference increases as the vapor temperature increases while just the opposite is true in Case 6.

Case #	Wall Thickness(mm)	Mesh Size	Filament Radius(mm)	Distance Between Filament Centers	Number of Screen Layers	Thickness of Fluid Layers(mm)
1	1.0150	400	0.0155	0.06919	2	0.03048
2	0.3968	400	0.0155	0.06919	2	0.03048
3	2.0300	400	0.0155	0.06919	2	0.03048
4	1.0150	250	0.0241	0.1198	2	0.03048
5	1.0150	100	0.0815	0.2937	2	0.03048
6	1.0150	400	0.0155	0.06919	1	---
7	1.0150	400	0.0155	0.06919	3	0.03048
8	1.0150	400	0.0155	0.06919	2	0.01524
9	1.0150	400	0.0155	0.06919	2	0.06096

Table I. Values of Parameters for Cases Considered in This Study

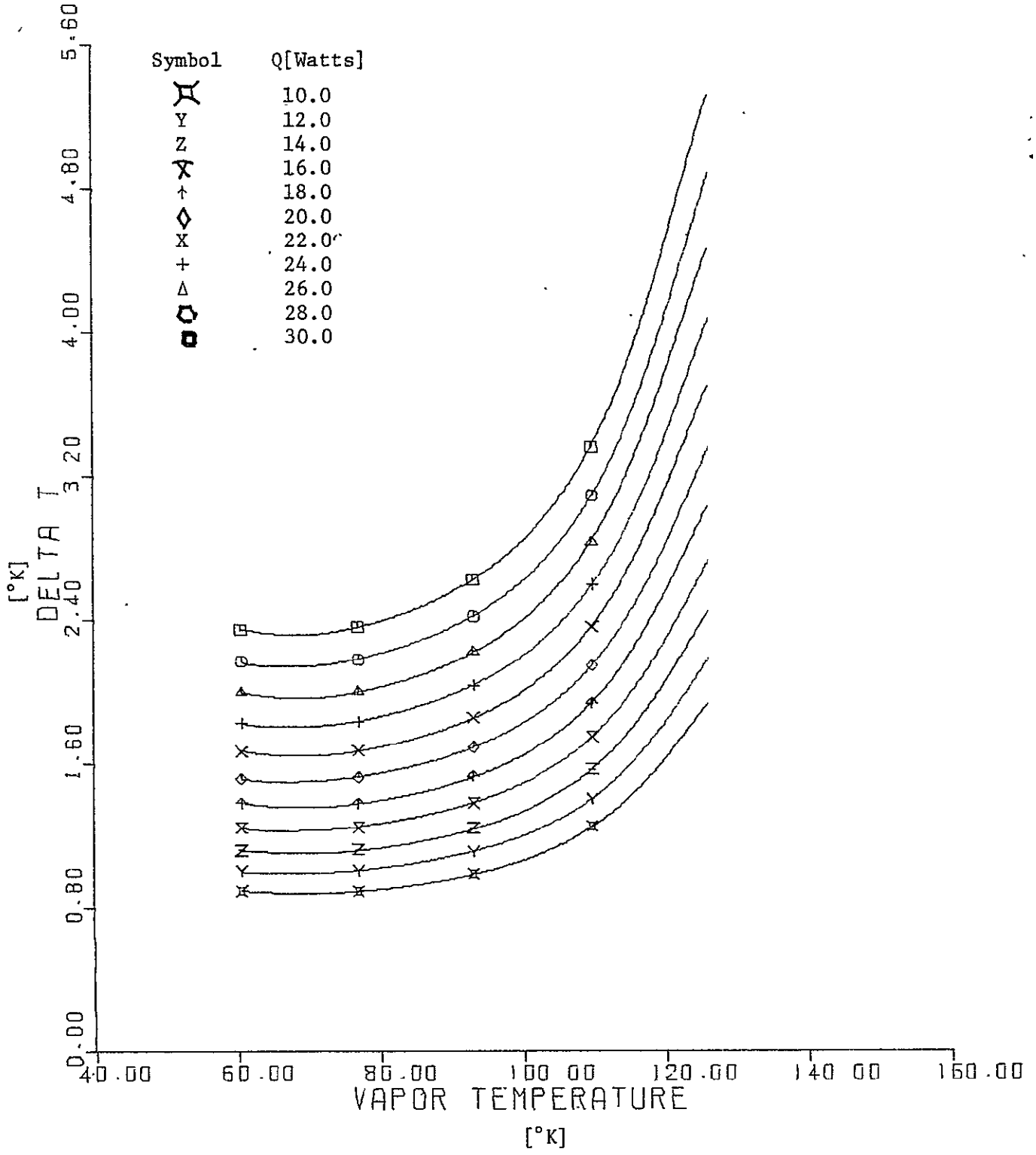

Figure 5. ΔT vs. T_V at constant Q - Case 1

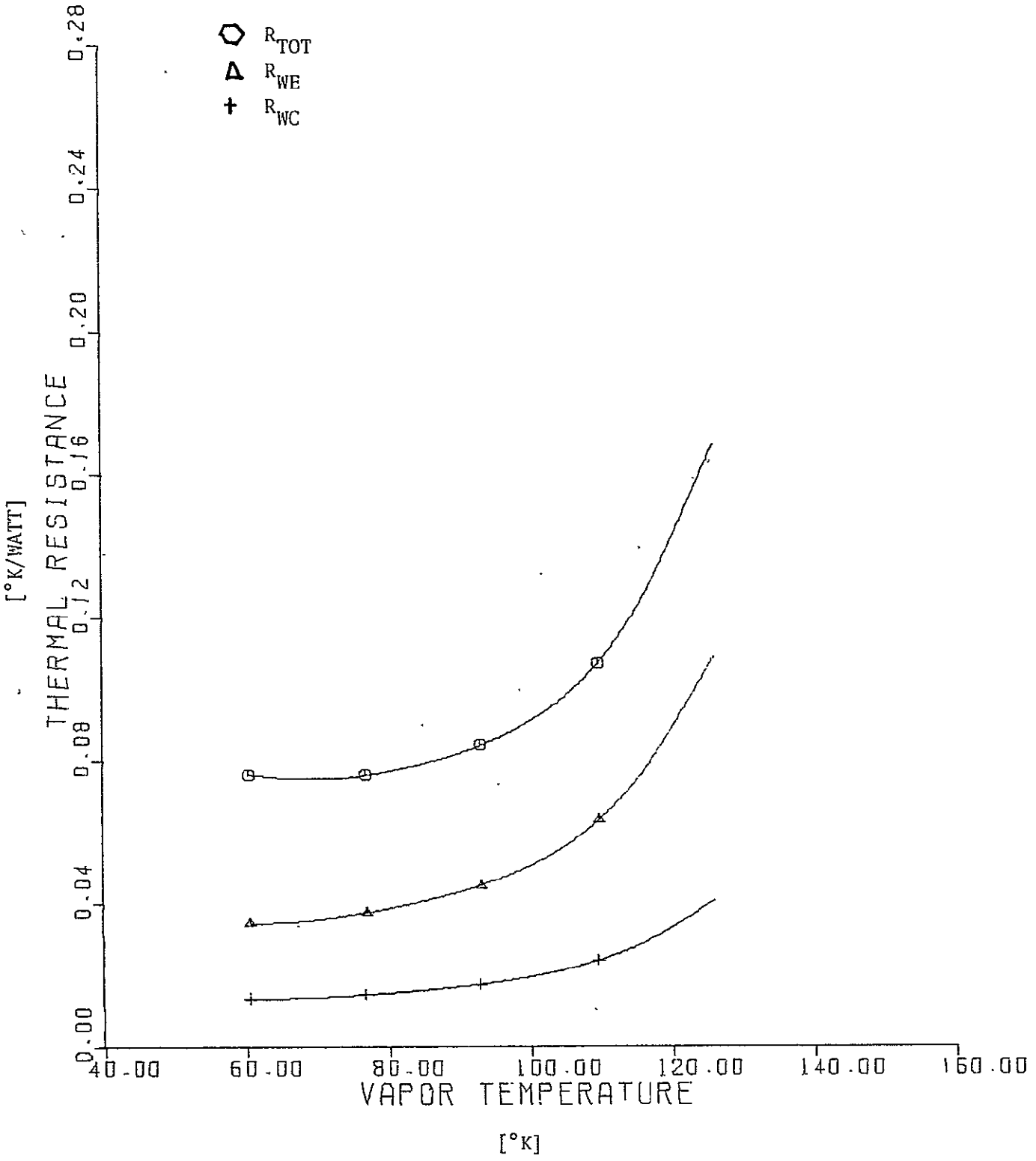

Figure 6. R_{TOT}, R_{WE}, R_{WC} vs. T_V for Q = 22 Watts - Case 1

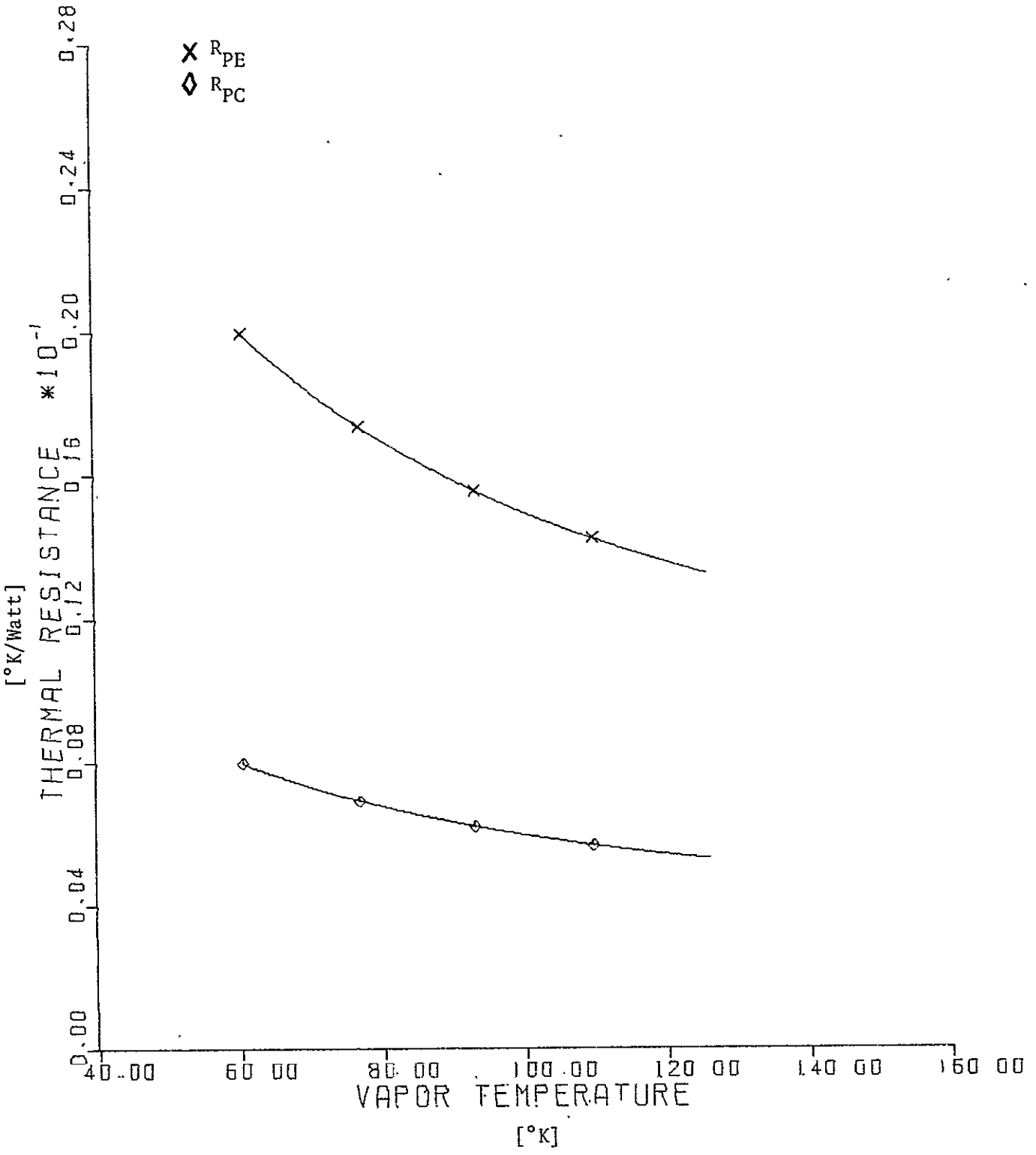

Figure 7. R_{PE}, R_{PC} VS. T_V for Q = 22 Watts - Case 1

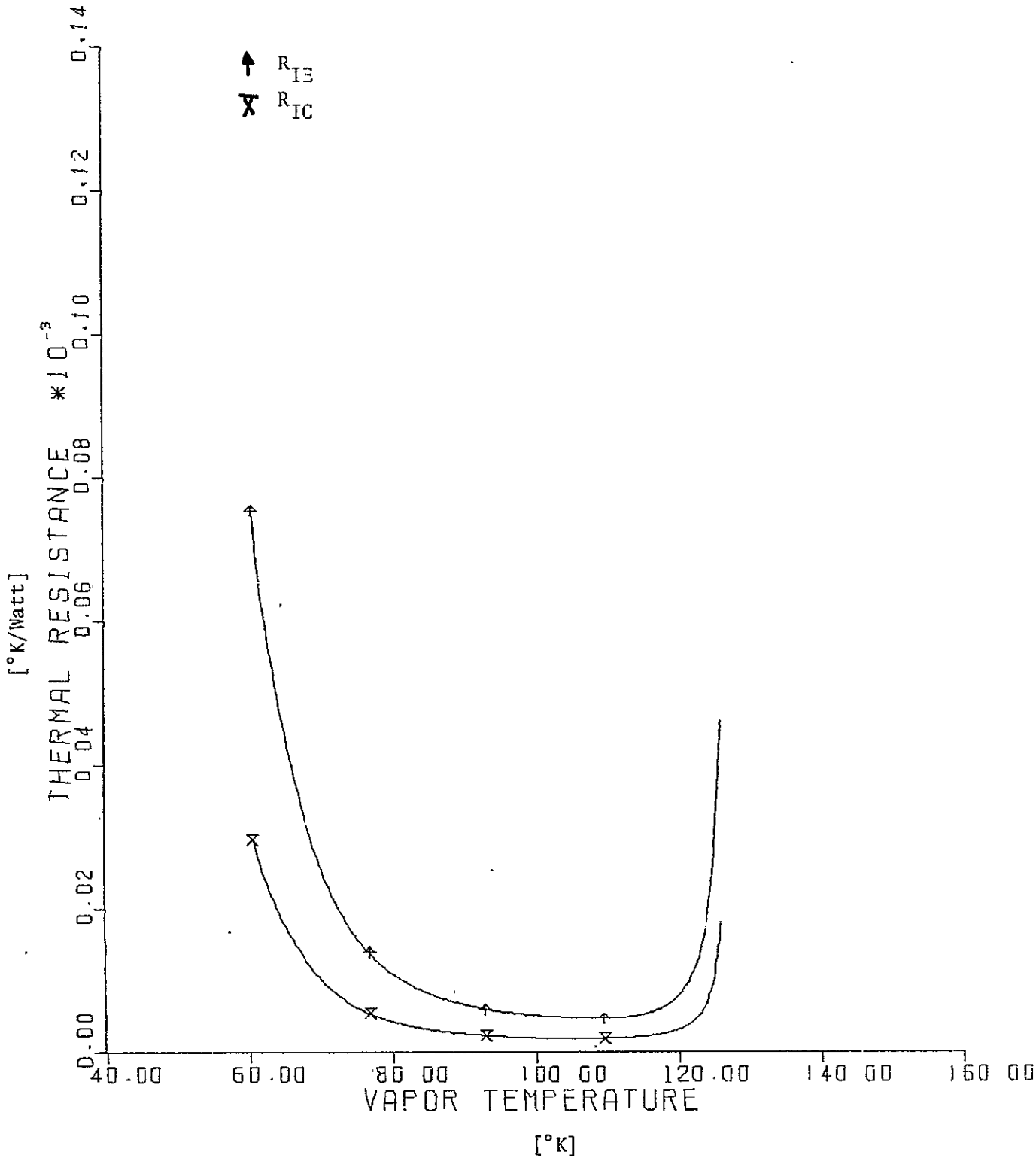

Figure 8. R_{IE}, R_{IC} VS. T_V for Q = 22 Watts - Case 1

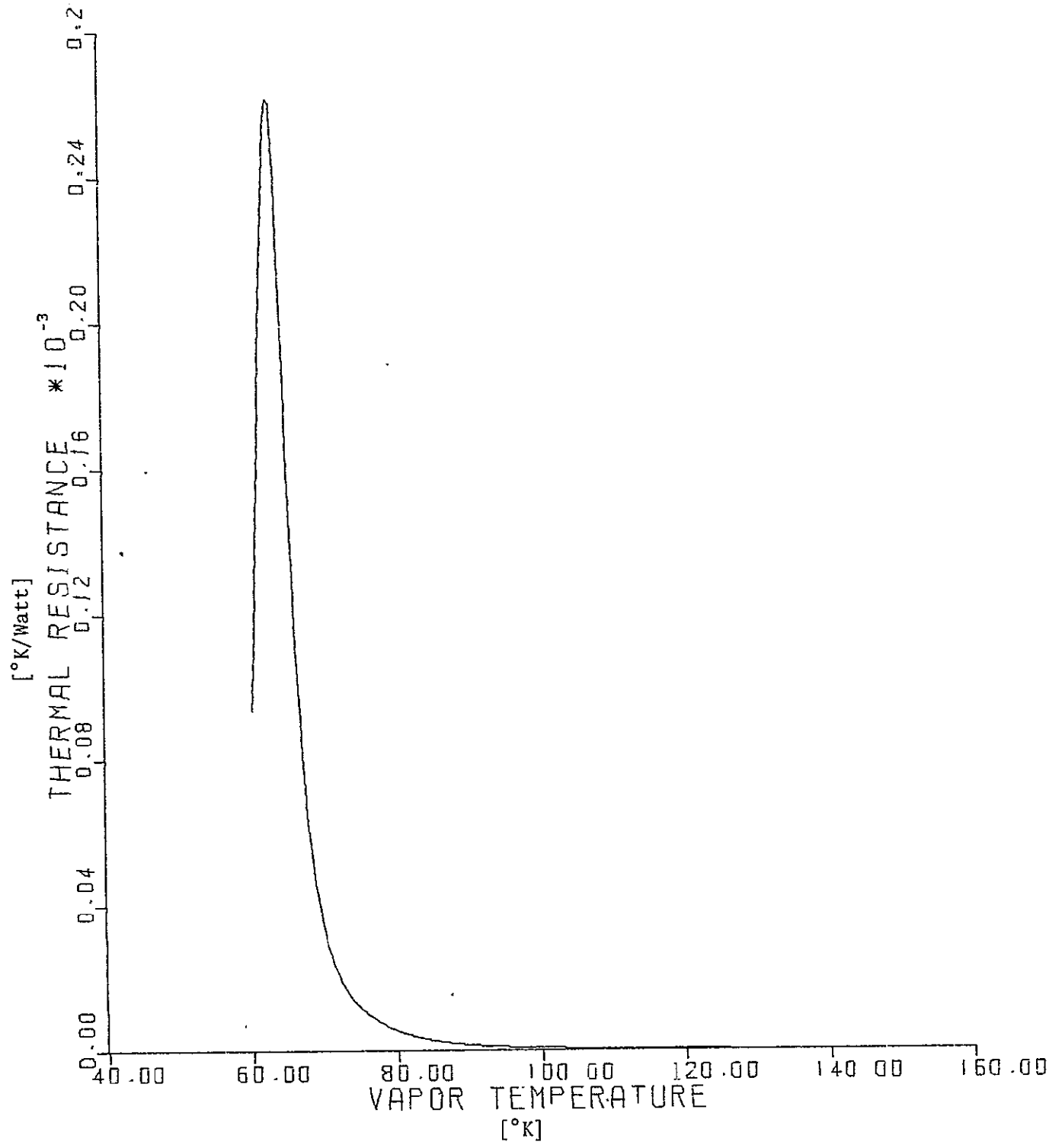

Figure 9. R_V VS. T_V for Q = 22 Watts - Case 1

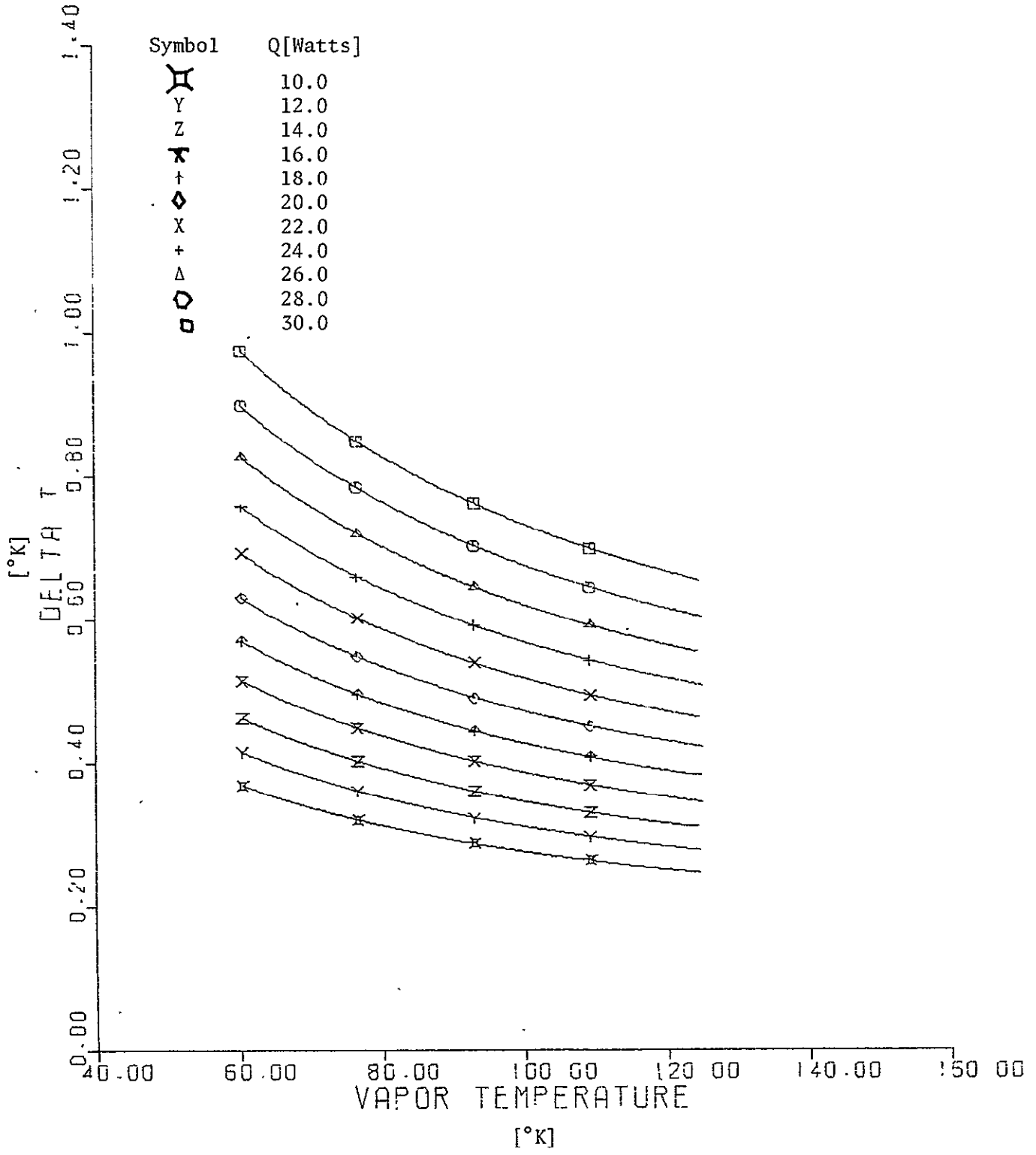

Figure 10. ΔT VS. T_V at Constant Q - Case 6

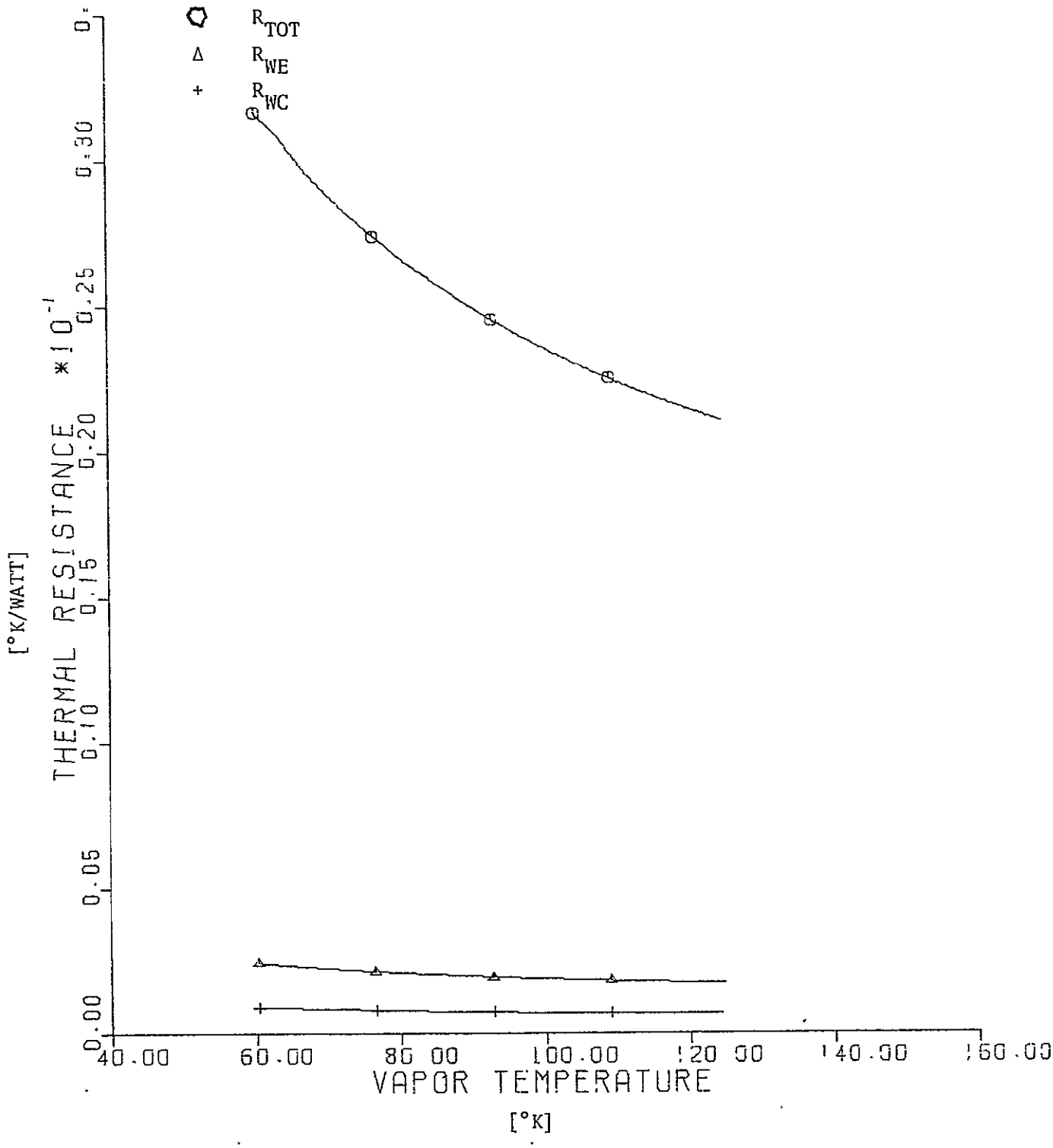

Figure 11. R_{TOT}, R_{WE}, R_{WC} VS. T_V for Q = 22 Watts - Case 6

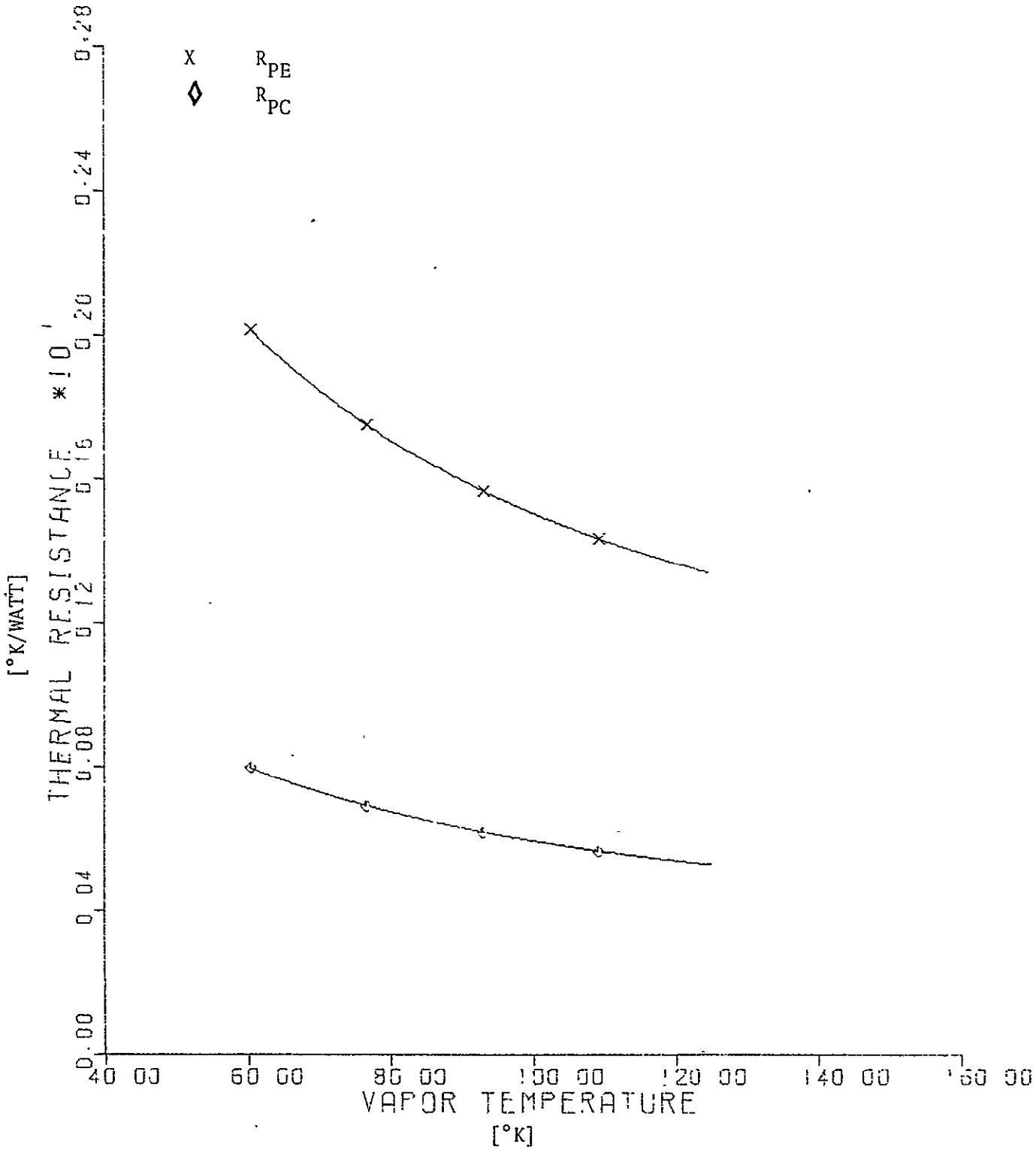

Figure 12. R_{PE}, R_{PC} VS. T_v for Q = 22 Watts - Case 6

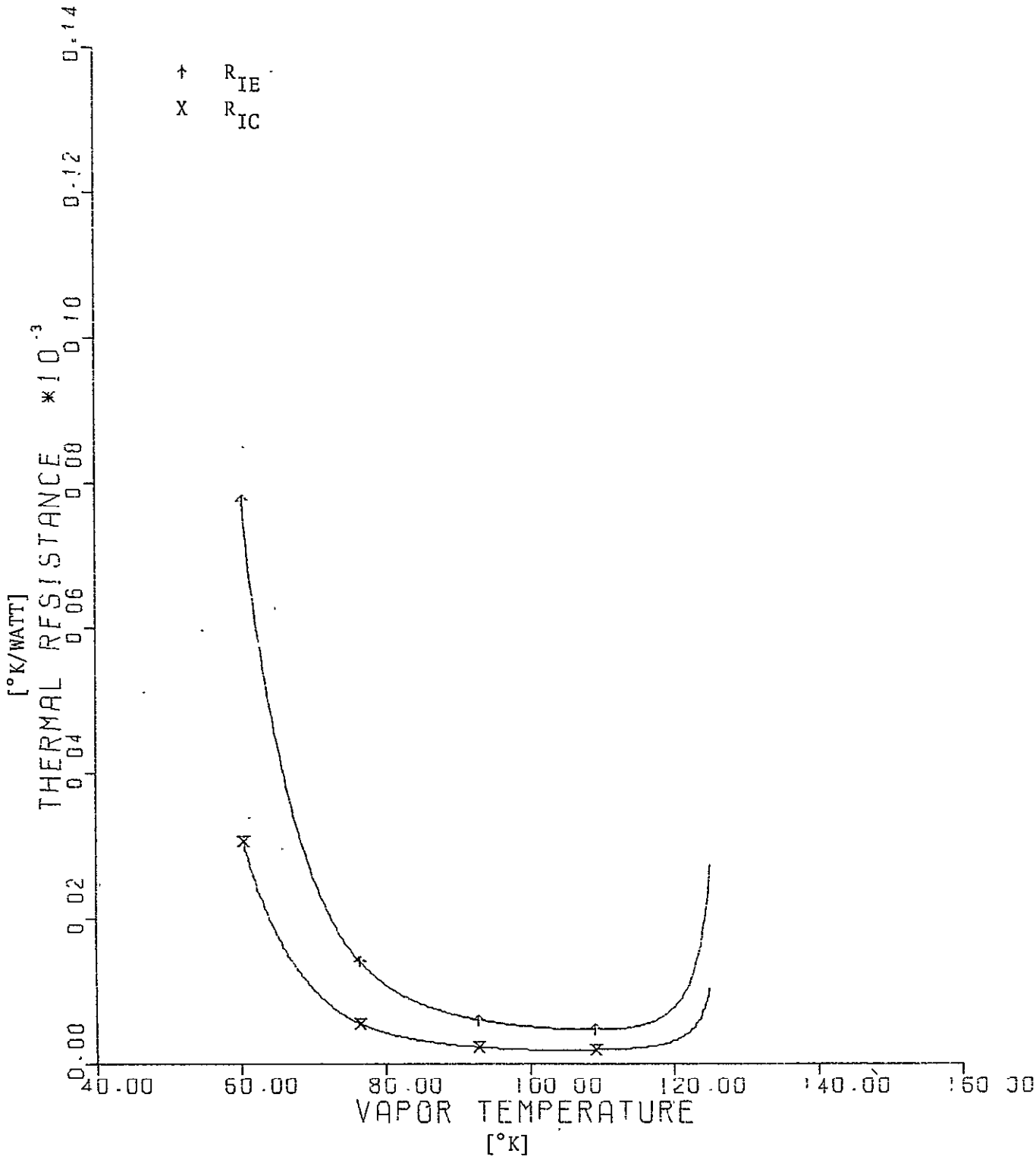

Figure 13. R_{IE}, R_{IC} VS. T_V for Q = 22 Watts - Case 6

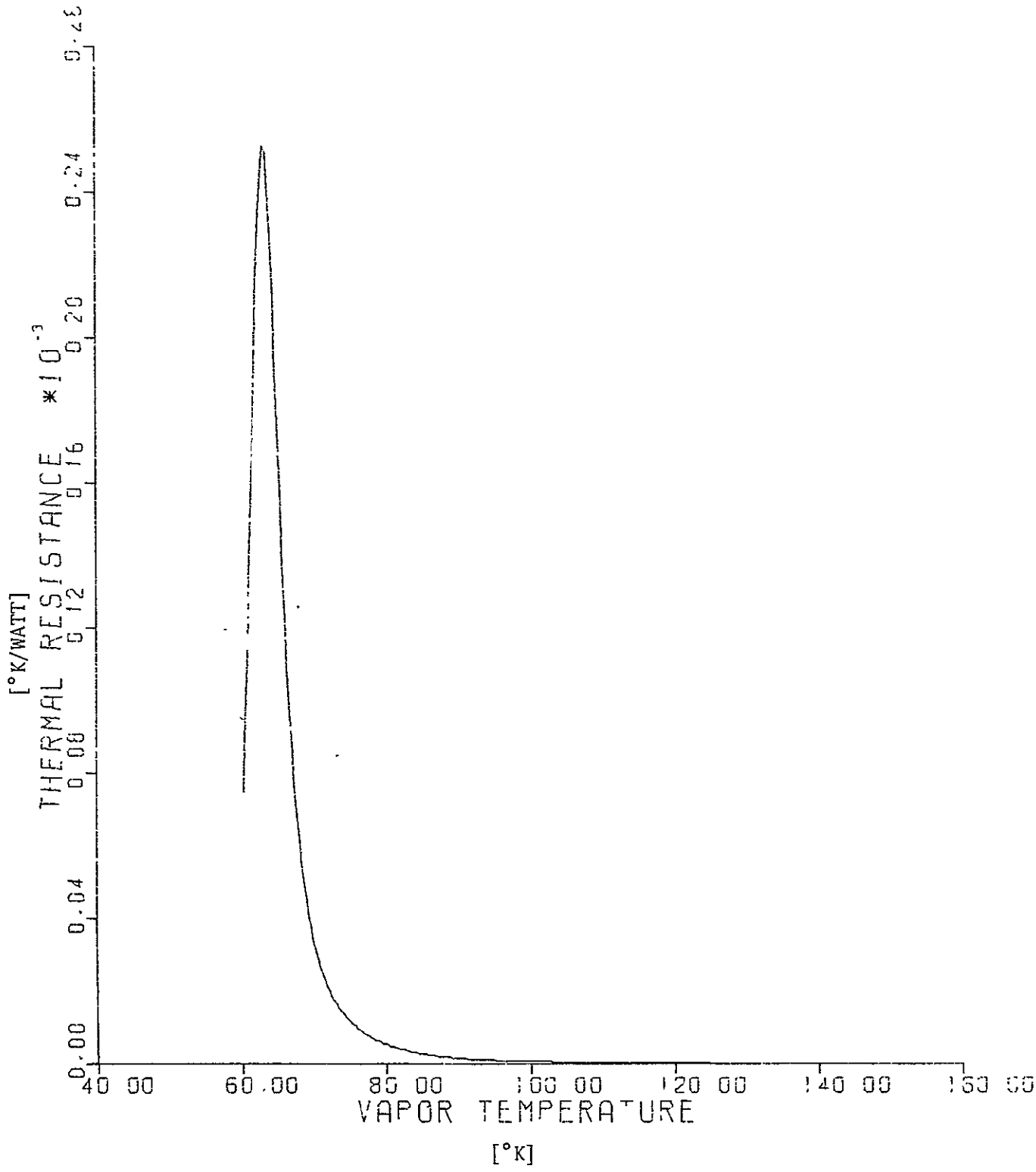

Figure 14. R_V VS. T_V for Q = 22 Watts - Case 6

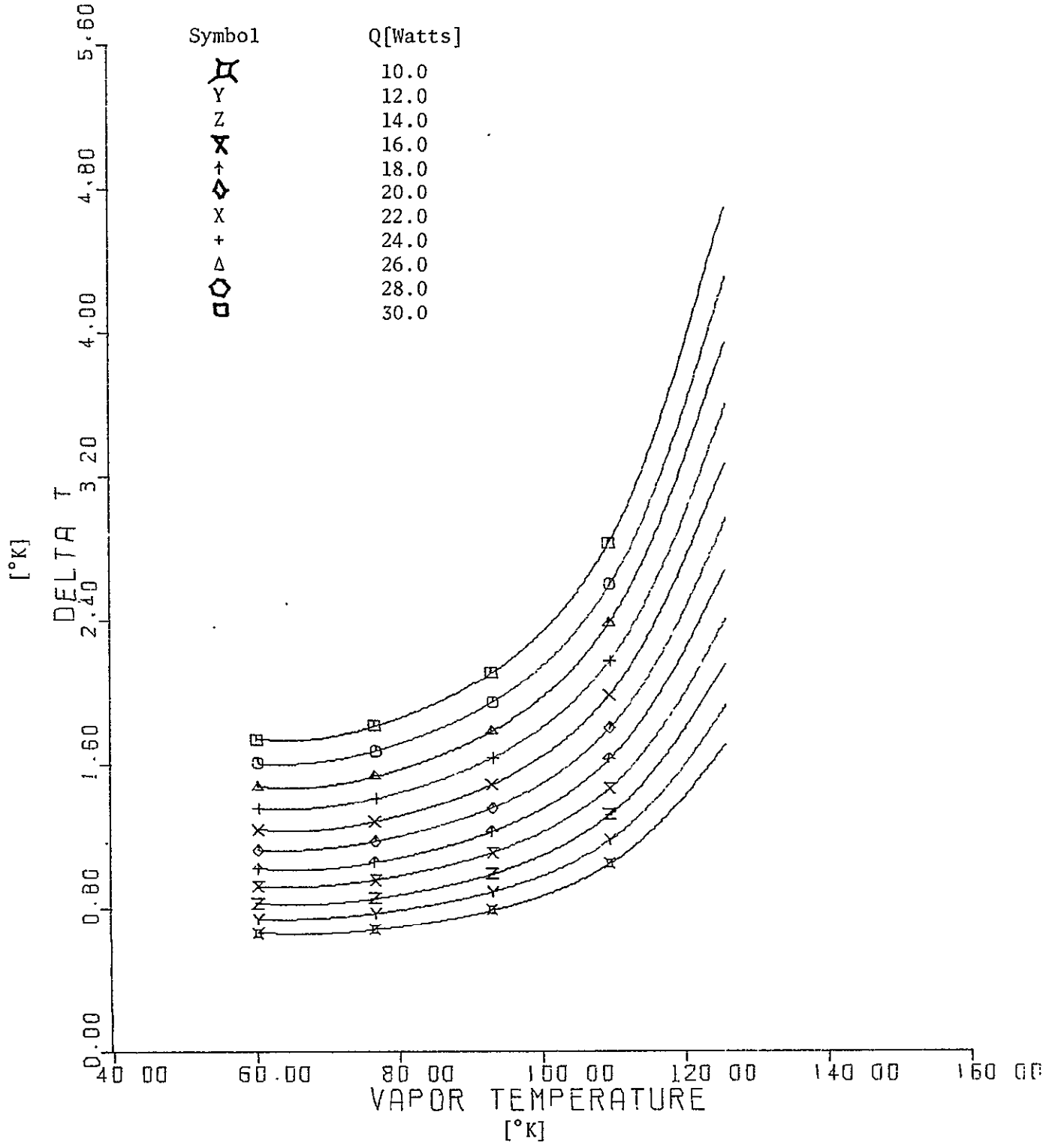

Figure 15. ΔT VS. T_V at Constant Q - Case 2

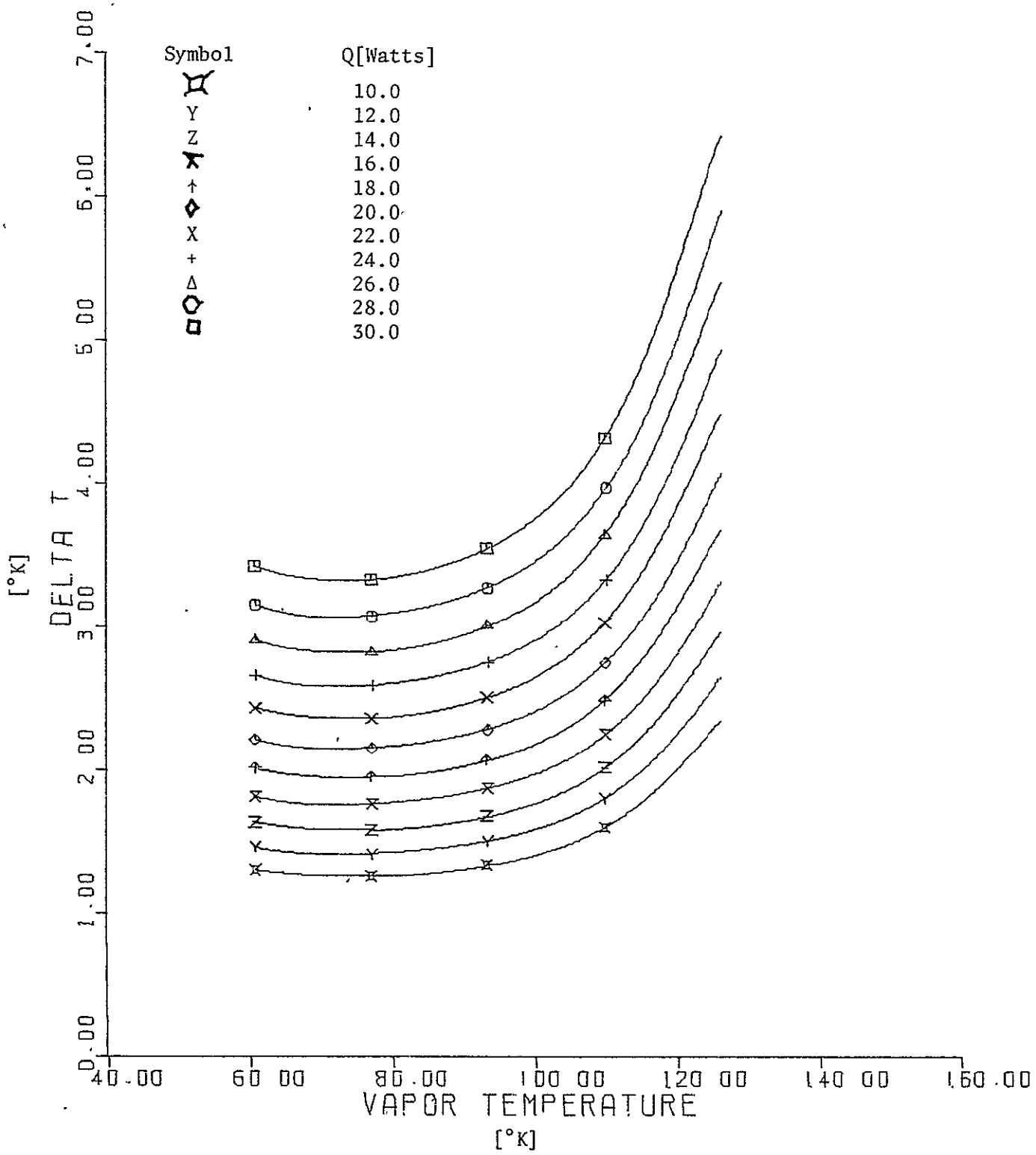

Figure 16. ΔT VS. T_V at Constant Q - Case 3

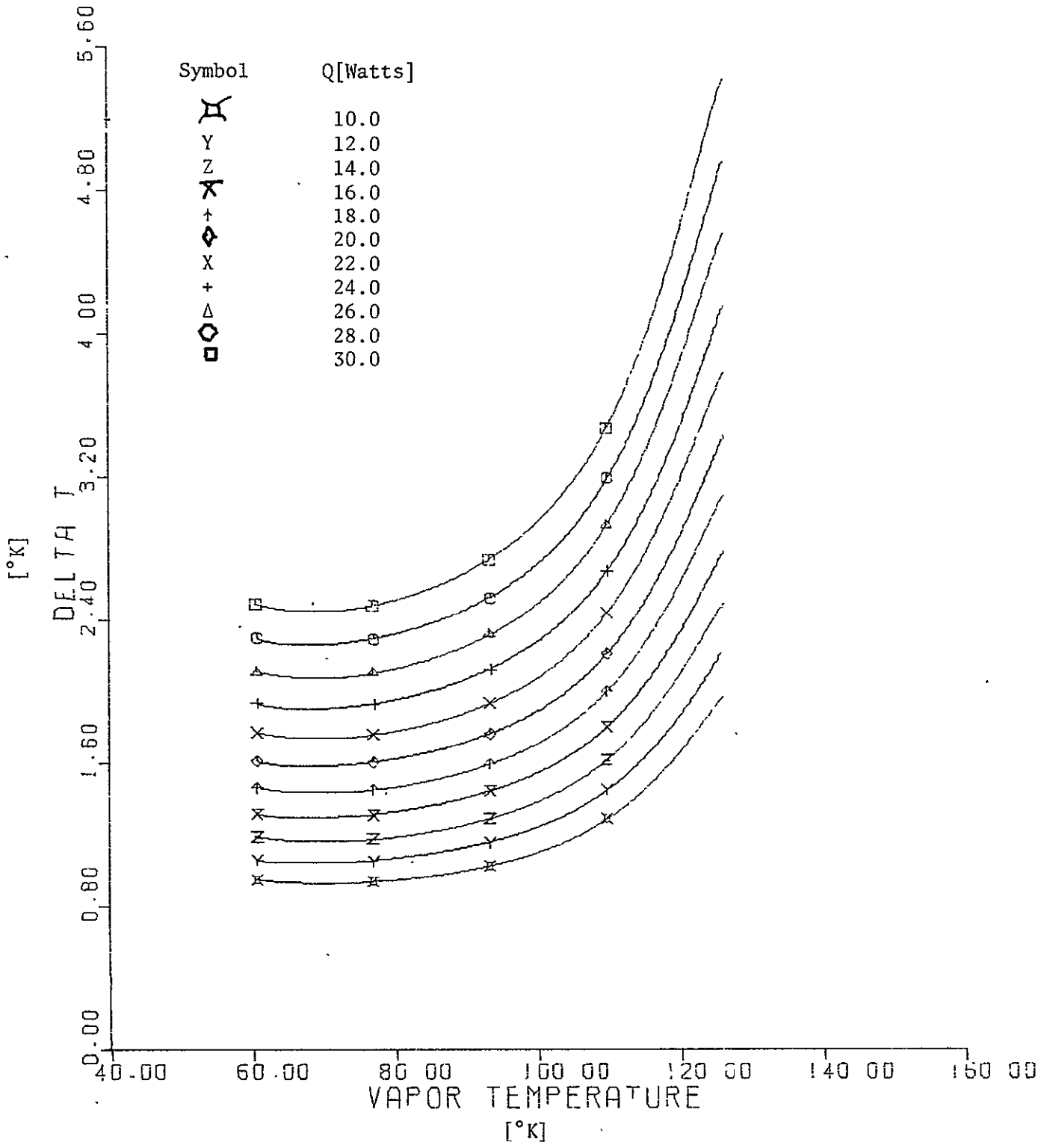

Figure 17. ΔT VS. T_V at Constant Q - Case 4

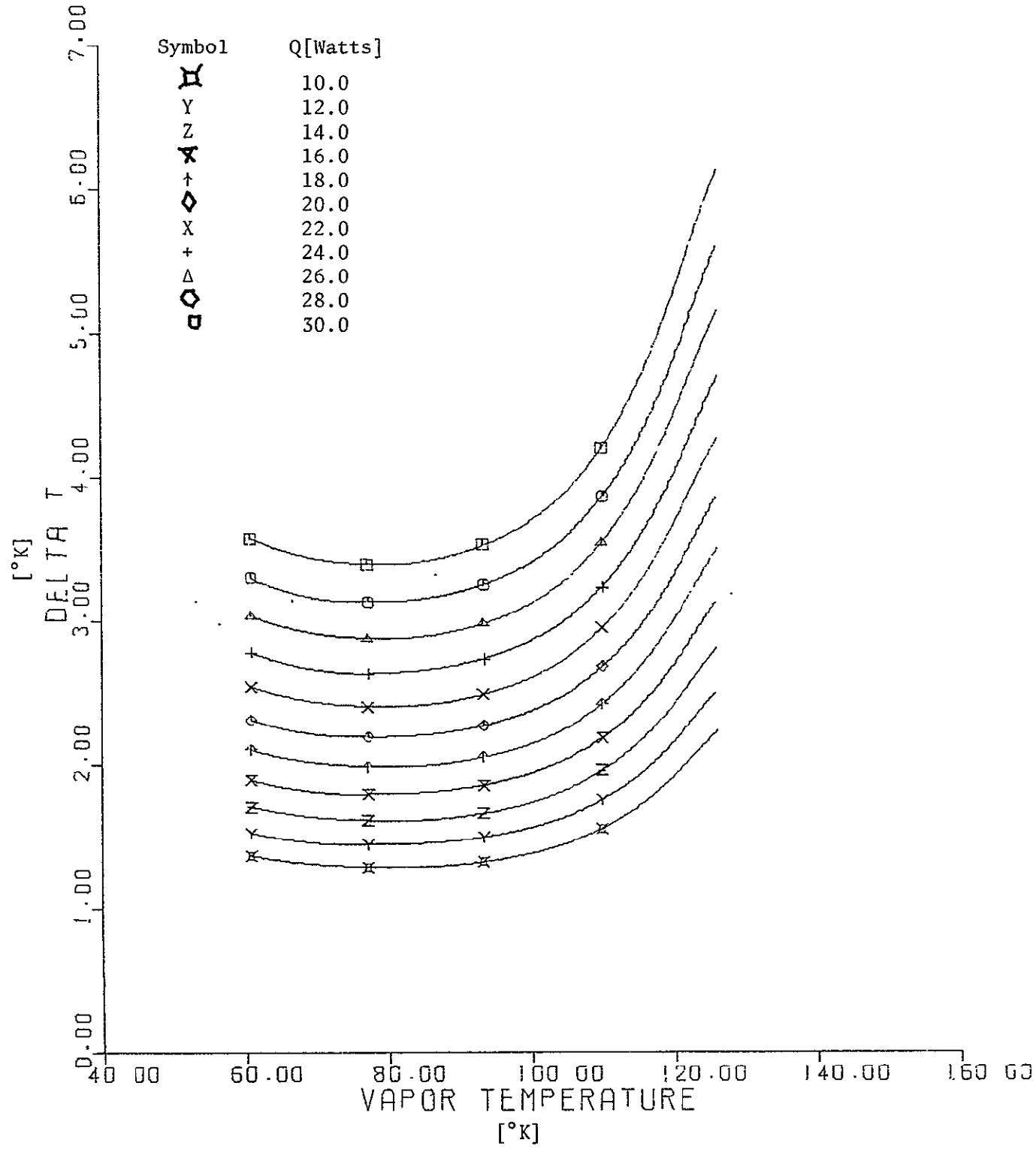

Figure 18. ΔT VS. T_V at Constant Q - Case 5

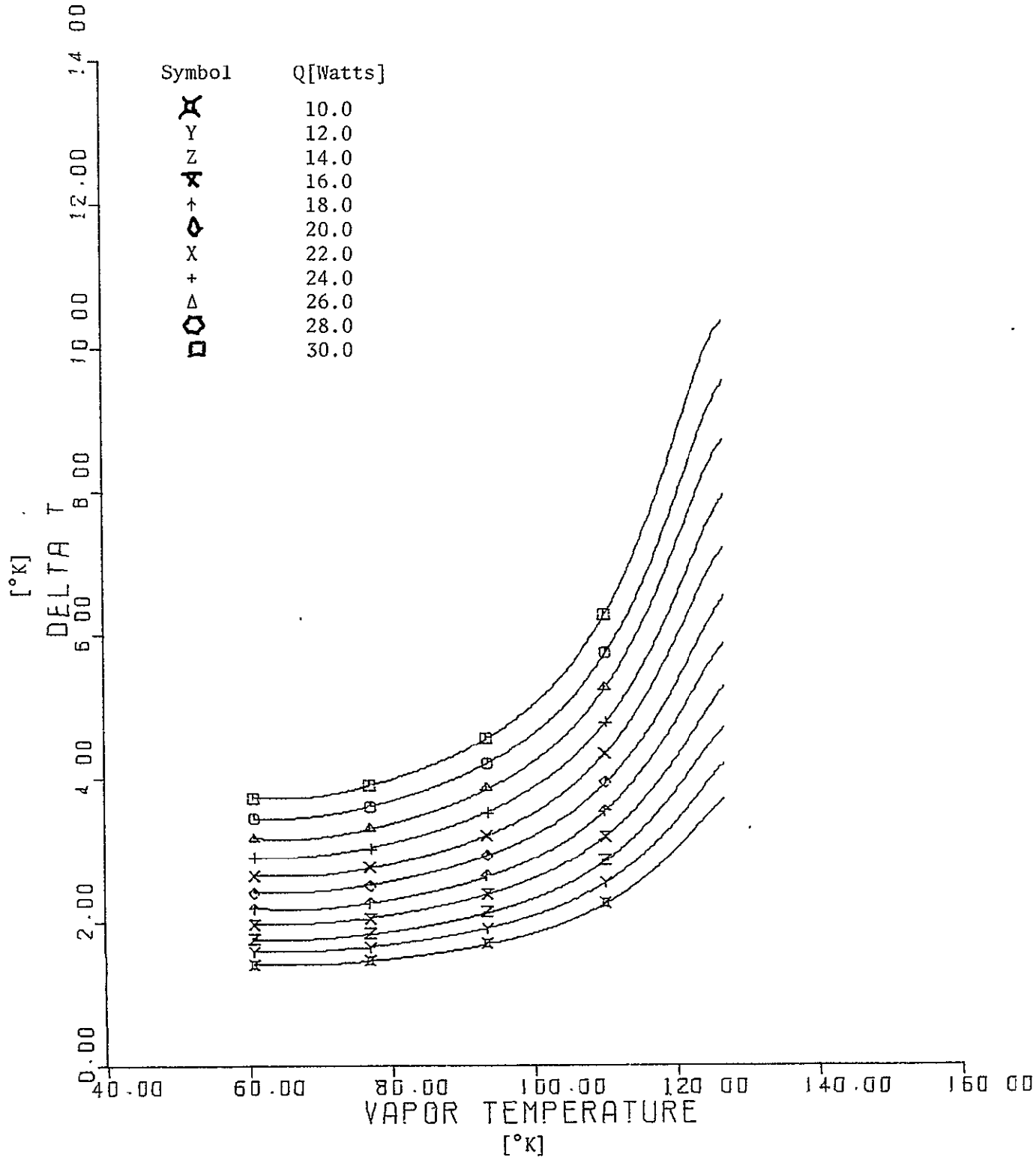

Figure 19. ΔT VS. T_V at Constant Q - Case 7

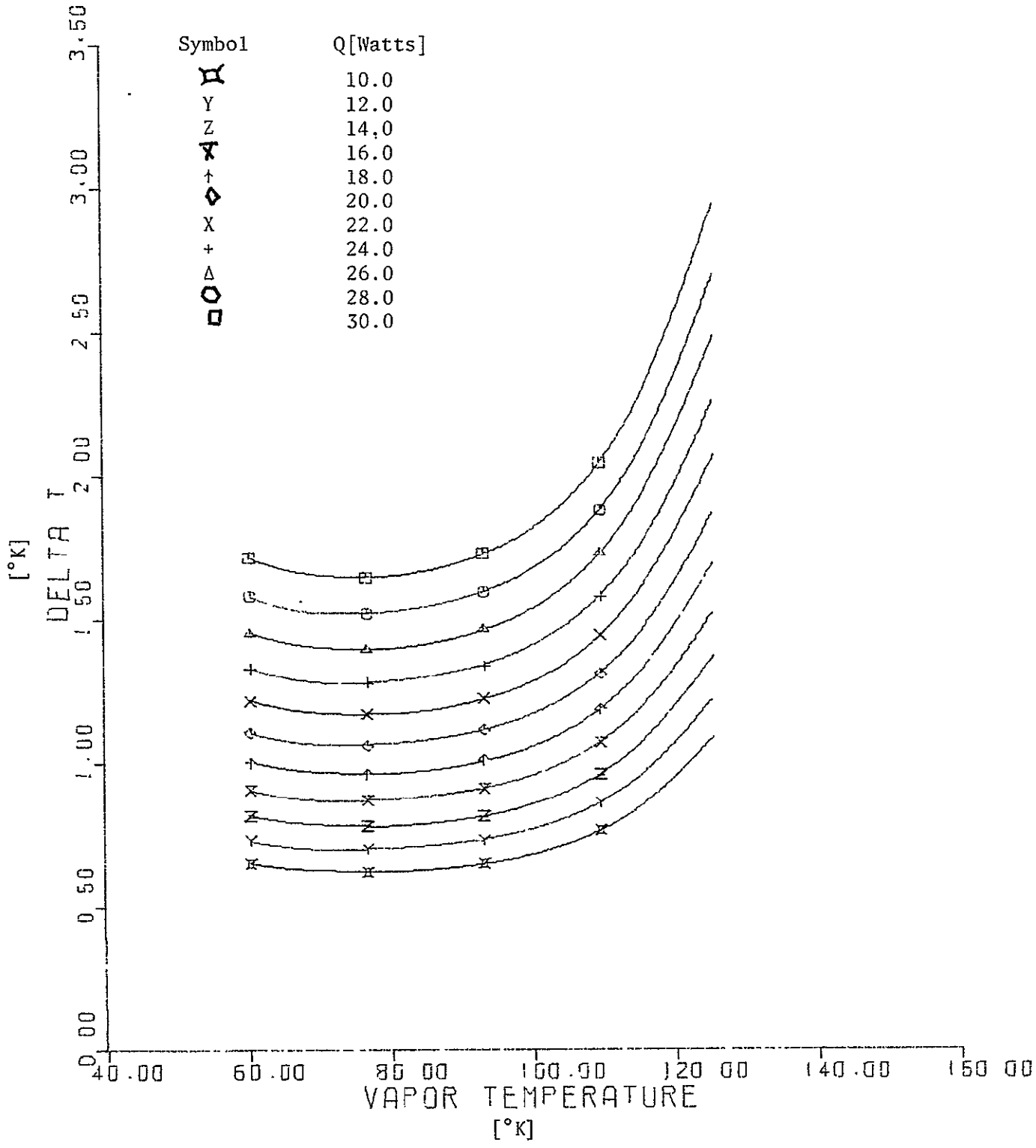

Figure 20. ΔT VS. T_V at Constant Q - Case 8

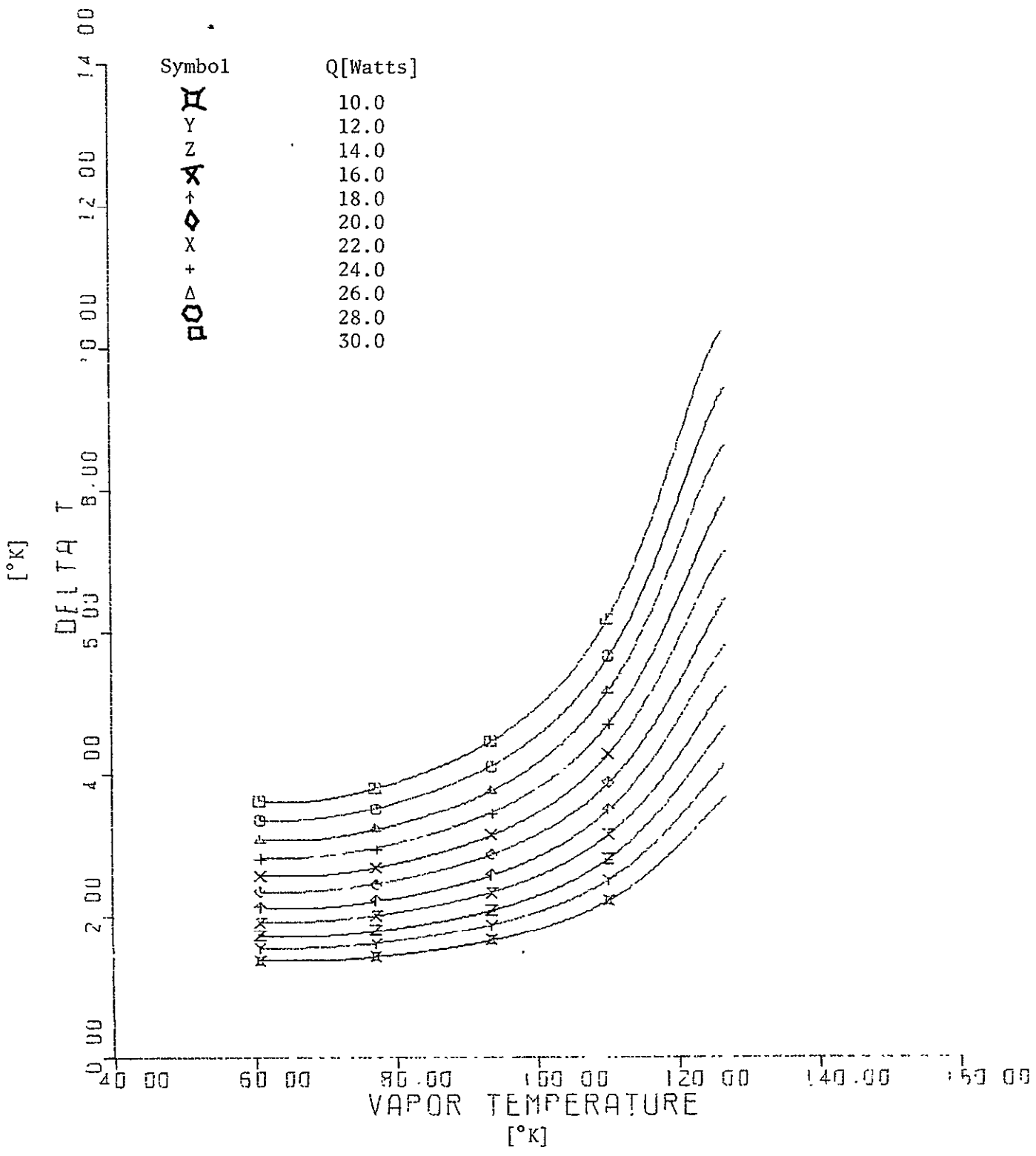

Figure 21. ΔT VS. T_V at Constant Q - Case 9

The reason for these different trends is that the thermal conductivity of liquid nitrogen decreases with increasing temperature while the conductivity of stainless steel increases with increase in temperature. In Case 1 the conductivity of the metal controls the effective conductivity of the fluid metal combination whereas in Case 6, the liquid nitrogen controls the effective conductivity of the combination.

Capillary Limitations

Writing momentum, energy and continuity equations for steady operation of the model heat pipe at capillary limited heat transfer and making the standard simplying assumptions the following equation is obtained.

$$\dot{Q}_{CL} = \frac{2N/r_p}{\frac{\bar{K}\ell_{eff}}{b\delta_T} + \frac{K_C L}{4n_C\delta_C}\left(\frac{1}{\ell_e} + \frac{1}{\ell_c}\right) + \frac{8\mu_V \rho_L \ell_{eff}}{\pi \mu_L \rho_V r_V^4}} \tag{32}$$

where

$\dot{Q}_{CL}$ = Capillary limited heat transfer rate

$N = \frac{\sigma h_{fg} \rho_L}{\mu_L}$ = "Heat Pipe Number"

σ = surface tension of liquid

h_{fg} = heat of vaporization

ρ_L = liquid density

μ_L = liquid dynamic viscosity

r_p = pore radius at evaporator surface

$\bar{K} = \frac{\delta_T}{\frac{n_A\delta_A}{K_A} + \frac{n_B\delta_B}{K_B}}$ = effective inverse permeability for slab based on approach velocity.

δ_T = total thickness of slab

n_A = number of layers of fine mesh in slab

n_B = number of layers of coarse mesh in slab

δ_A = thickness of a single layer of material A

δ_B = thickness of a single layer of material B

K_A = inverse permeability for material A based on approach velocity

K_B = inverse permeability for material B based on approach velocity

ℓ_{eff} = effective length of liquid path in slab

b = width of slab

K_c = inverse permeability for material at evaporator and condenser surfaces based on approach velocity

L = average distance traveled by liquid in circumferential capillary structure at evaporator or condenser (approximately 45° arc)

n_c = number of layers of capillary material on circumference

δ_c = thickness of a single layer of material C

ℓ_e = axial length of evaporator section

ℓ_c = axial length condenser section

μ_V = dynamic viscosity of vapor

ρ_V = density of vapor

r_V = hydraulic radius of vapor space

Approximately one hundred different capillary arrangements were studied in order to determine capillary limitations. Table II shows geometric parameters for six of the combinations examined. Capillary limitations as a function of vapor temperature are shown in Figure 22 for each of the combinations listed in Table II.

Transient Analog Computer Studies

A rather simplified transient model of a cryogenic slab type heat pipe with radiator connected is shown in Figure 23. Due to limited analog computer capacity relatively few nodes were used. The equations written for this model are:

$$Q_e = \frac{2\pi \ell_e k_p}{\ln (r_A/r_B)} (T_e - T_1) + \frac{\rho_p c_{pe} V_p}{2} \frac{dT_e}{d\theta} \qquad (33)$$

Table II. Description of Composite Wick Systems Considered in this Study

Wick Composition Number	Screen Mesh Size			Number of Layers			Screen Thickness - m			Total Thickness of Slab - m
	A	B	C	n_A	n_B	n_C	$\delta_A \times 10^4$	$\delta_B \times 10$	$\delta_C \times 10^4$	$\delta_T = n_A\delta_A + n_B\delta_B$
1	250	100	250	2	8	1	0.867	0.314	0.866	2.68
2	400	50	400	2	5	1	0.744	0.448	0.744	2.39
3	400	30	400	2	4	1	0.744	0.622	0.744	2.64
4	400	30	400	4	5	2	0.744	0.622	0.744	3.41

Wick Composition Number	Wire Diameter "C" Layer m x 10^4	Pore Radius "C" Layer m x 10^4	Inverse Permeability-$1/m^2$			Effective Permeability - $1/m^2$
			$K_A \times 10^{-9}$	$K_B \times 10^{-7}$	$K_C \times 10^{-9}$	$\bar{K} = \delta_T / \left(\frac{n_A\delta_A}{K_A} + \frac{n_B\delta_B}{K_B} \right) \times 10^{-7}$
1	0.482	0.359	58.4	2,610	58.4	2,716
2	0.311	0.191	163	195	163	207
3	0.311	0.191	163	63.5	163	67.3
4	0.311	0.191	163	63.5	163	69.6

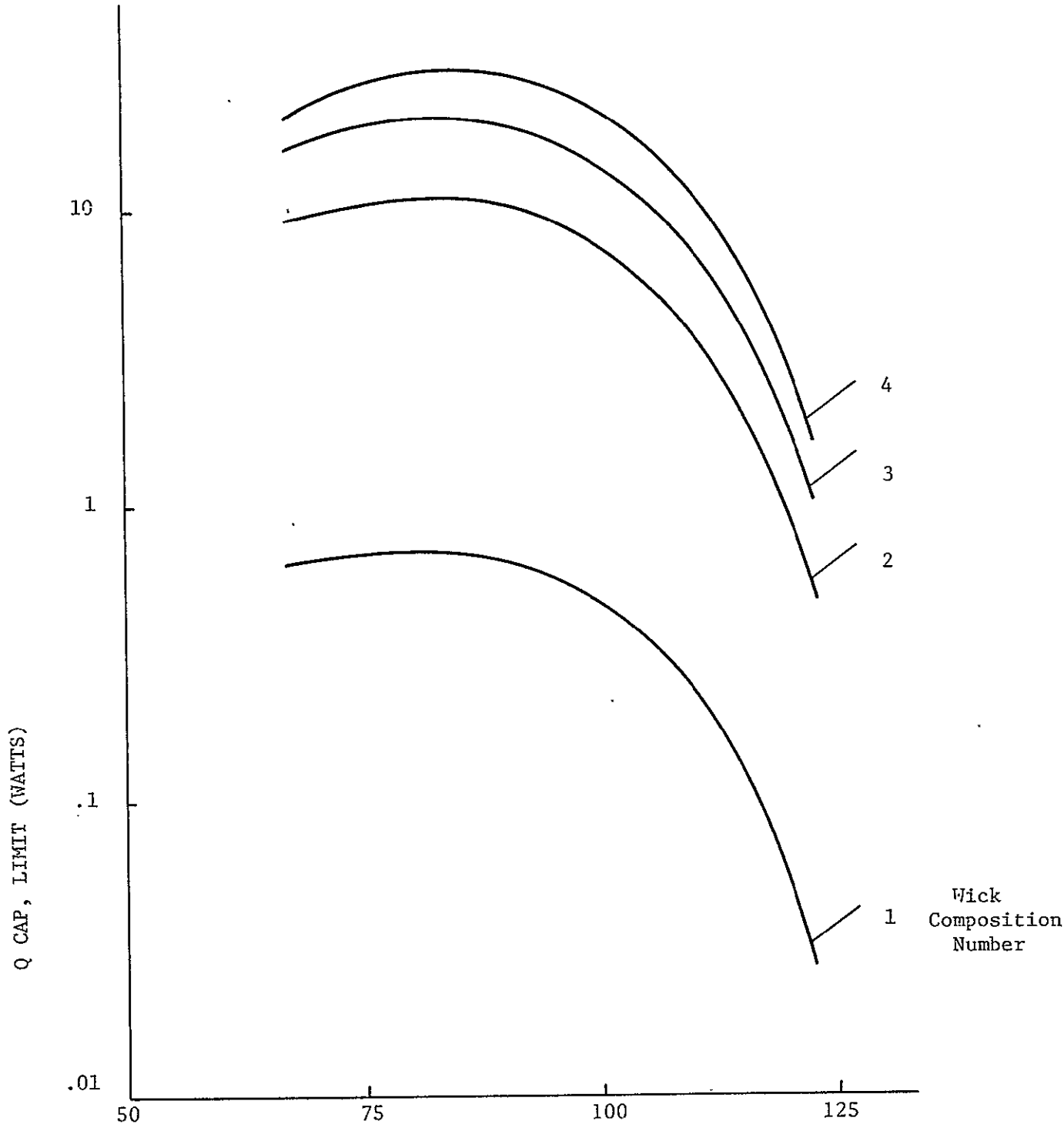

Figure 22. VAPOR TEMPERATURE (°K)

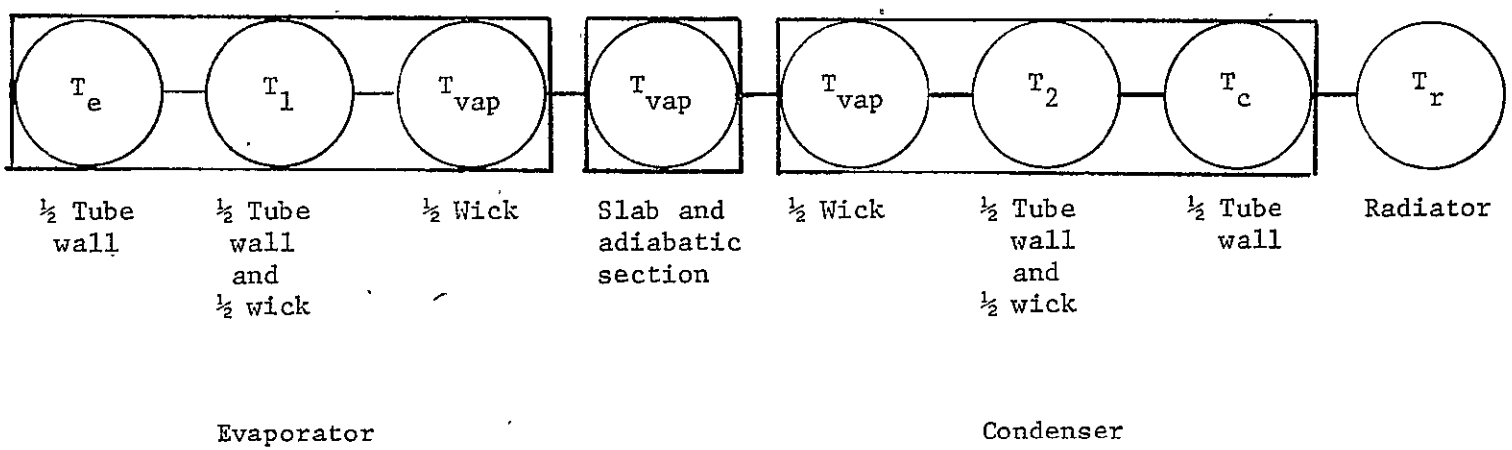

Figure 23 Analog Model

$$\frac{dT_1}{d\theta} = \frac{4\pi\, \ell_e\, k_p}{[\rho_p c_{pe} V_p + \rho_w c_{we} V_p] \ln (r_A/r_B)} (T_e - T_1)$$

$$+ \frac{4\pi\, \ell_e\, k_w}{[\rho_p c_{pe} V_p + \rho_w c_{we} V_w] \ln (r_B/r_C)} (T_{vap} - T_1) \quad (34)$$

$$\frac{dT_{vap}}{d\theta} = \frac{4\pi\, k_w\, \ell_e}{[\rho_w c_{we} V_w + \rho_w c_{wc} V_w + 2m_a c_a] \ln (r_B/r_C)} (T_1 - T_{vap})$$

$$+ \frac{4\pi\, k_w\, \ell_c}{[\rho_w c_{we} V_w + \rho_w c_{wc} V_w + 2m_a c_a] \ln (r_B/r_C)} (T_2 - T_{vap}) \quad (35)$$

$$\frac{dT_2}{d\theta} = \frac{4\pi\, k_w\, \ell_c}{[\rho_p c_{pc} V_p + \rho_w c_{wc} V_w] \ln (r_B/r_C)} (T_{vap} - T_2)$$

$$+ \frac{4\pi\, k_p\, \ell_c}{[\rho_p c_{pc} V_p + \rho_w c_{wc} V_w] \ln (r_A/r_B)} (T_c - T_2) \quad (36)$$

$$\frac{dT_c}{d\theta} = \frac{4\pi\, k_p\, \ell_c}{\rho_p c_{pc} V_p \ln(r_A/r_B)} (T_2 - T_c) + \frac{4\pi\, r_a\, \ell_c}{\rho_p c_{pc} V_p R_c} (T_r - T_c) \quad (37)$$

$$\frac{dT_r}{d\theta} = \frac{2\pi\, r_a\, \ell_c}{m_r c_r} (T_c - T_r) - \frac{\varepsilon A_r \sigma}{m_r c_r} T_r^4 + \frac{Q_{space}}{m_r c_r} \quad (38)$$

Limiter

$$(T_1 - T_{vap}) \leq \frac{Q_{CL} \ln (r_B/r_C)}{2\pi\, k_w\, \ell_e}$$

where

A_r = area of radiator

c_a = effective specific heat of adiabatic section and slab

c_p = specific heat of pipe material

c_r = specific heat of radiator

m_a = mass of adiabatic section and slab

m_r = mass of radiator

Q_e = heat flux into evaporator

Q_{space} = heat flux into radiator

Q_r = net heat flux from radiator

R_c = contact resistance between node c and node r

T_e = temperature node e

T_1 = temperature node 1

T_{vap} = temperature node vap

T_2 = temperature node 2

T_c = temperature node c

T_r = temperature node r

${}_eV_p$ = volume of pipe material in evaporator

${}_cV_p$ = volume of pipe material in condensor

${}_eV_w$ = volume of wick material in evaporator

${}_cV_w$ = volume of wick material in condensor

ε = emmissivity of radiator

ρ_p = density of pipe material

ρ_w = effective density of wick and working fluid

σ = Stefan-Boltzman constant

θ = time

The limiter equation allows one to include the capillary limitation in computations.

Figure 24 shows a schematic of the analog computer circuit. Note that inclusion of the radiator introduces non-linear terms in the equation. However, these non-linear terms have thus far caused no difficulties in the computations.

Figures 25, 26, and 27 show sample results of some computations performed for a nitrogen heat pipe of configuration. Figure 25 shows performance for a step change of 5°K in the evaporator temperature. Notice that heat transfer at the hot end (Q_e) is limited for some time due to capillary limitations. The system has essentially stabilized after 60 seconds. Figure 26 shows how all parameters vary for a relatively fast sine wave. Notice that the capillary limitation considerably affects heat transfer through the evaporator. As expected, the computations indicate progressively smaller oscillations in temperature as one moves away from the evaporator and finally the radiator increases with time but oscillates very little. There is a considerable phase shift between oscillations in different temperatures. Figure 27 shows the system changes for a relatively slow variation in evaporator temperature. Evaporator heat transfer is again limited by capillary restrictions. The amplitude of temperature oscillations tends to be more uniform throughout the pipe than in the case where fast oscillations were considered. There are large phase shifts.

Transient Digital Computer Studies

The analog computer program described above is limited to small transients and thus is of limited use. For this reason a digital computer program is now being developed to handle transient computations. The

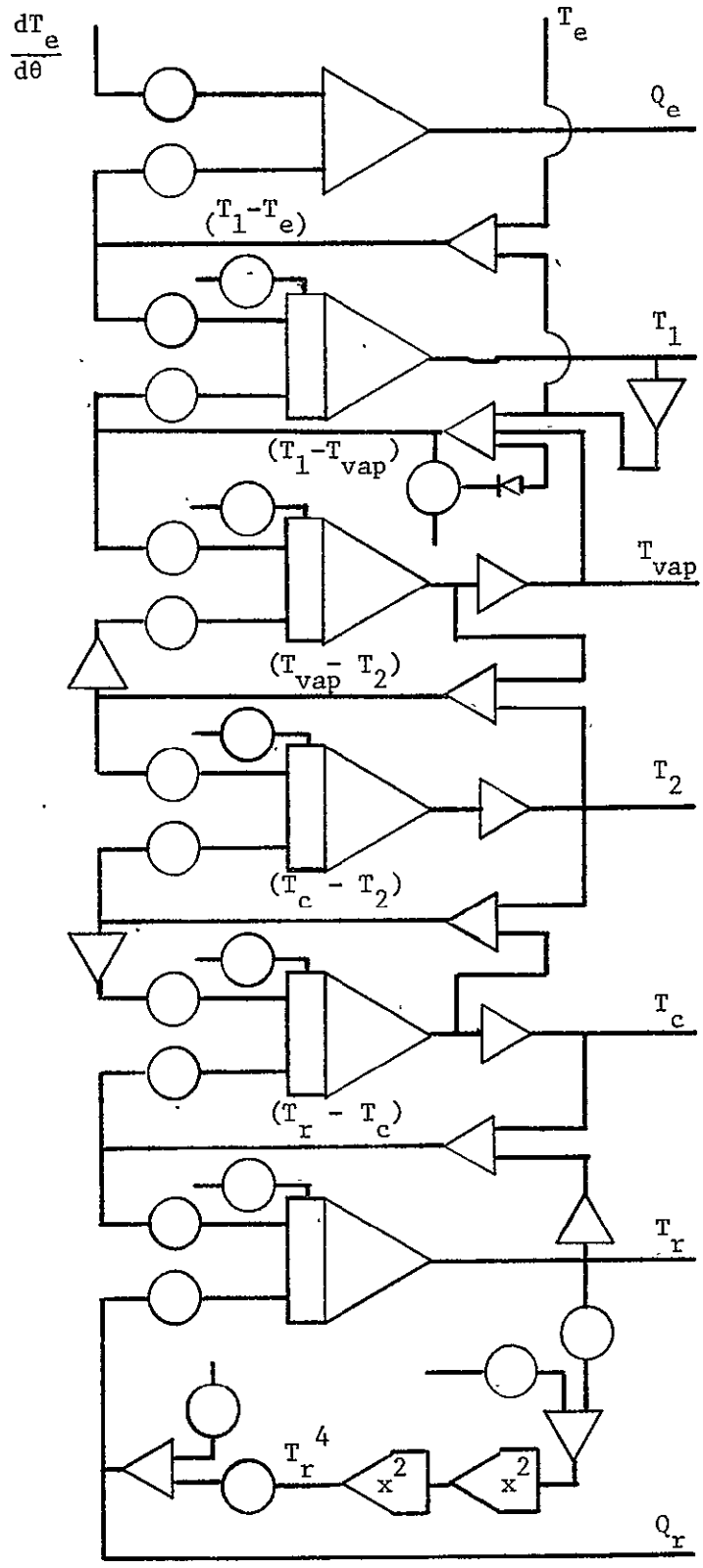

Figure 24. Analog Circuit

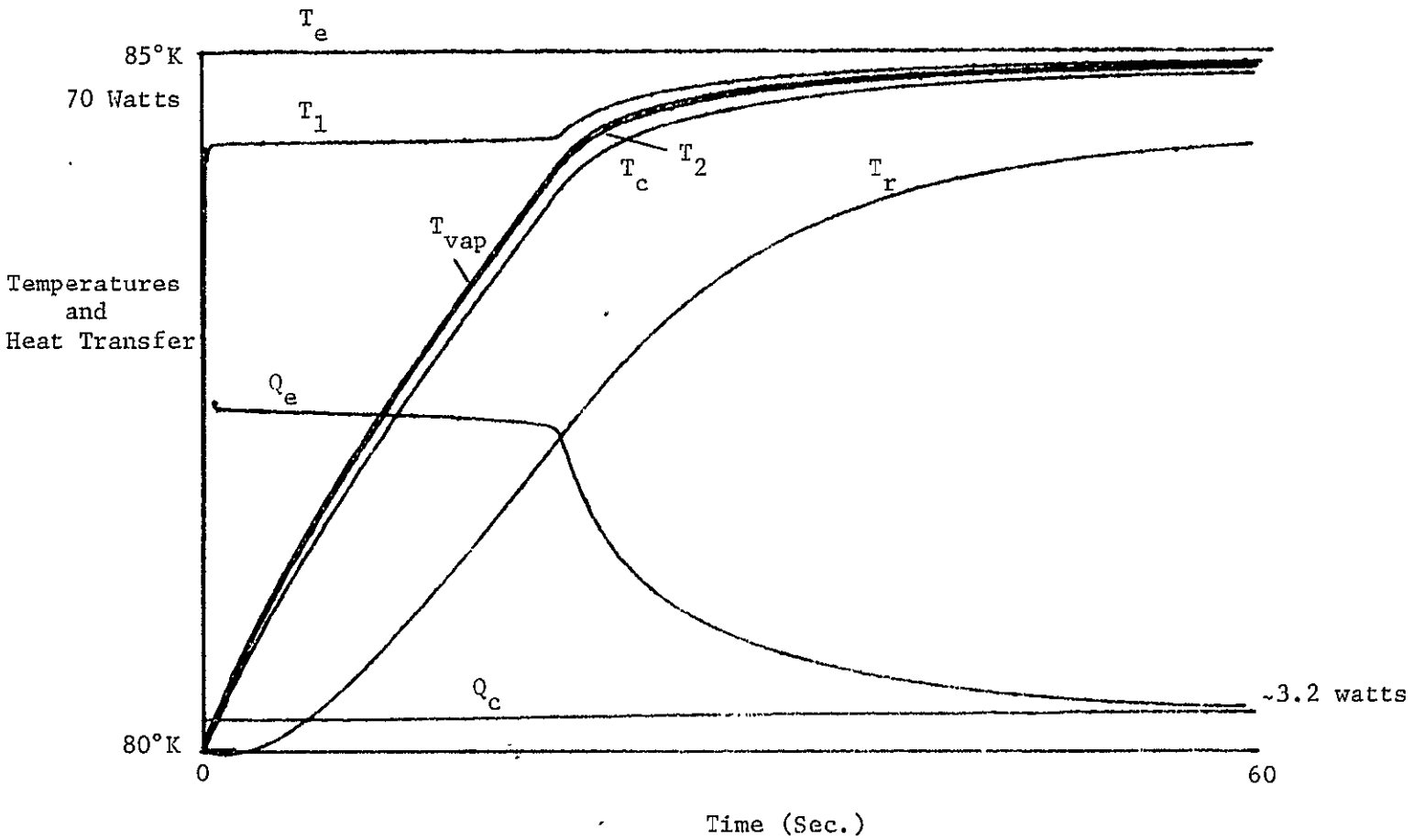

Figure 25. Step Temperature Change

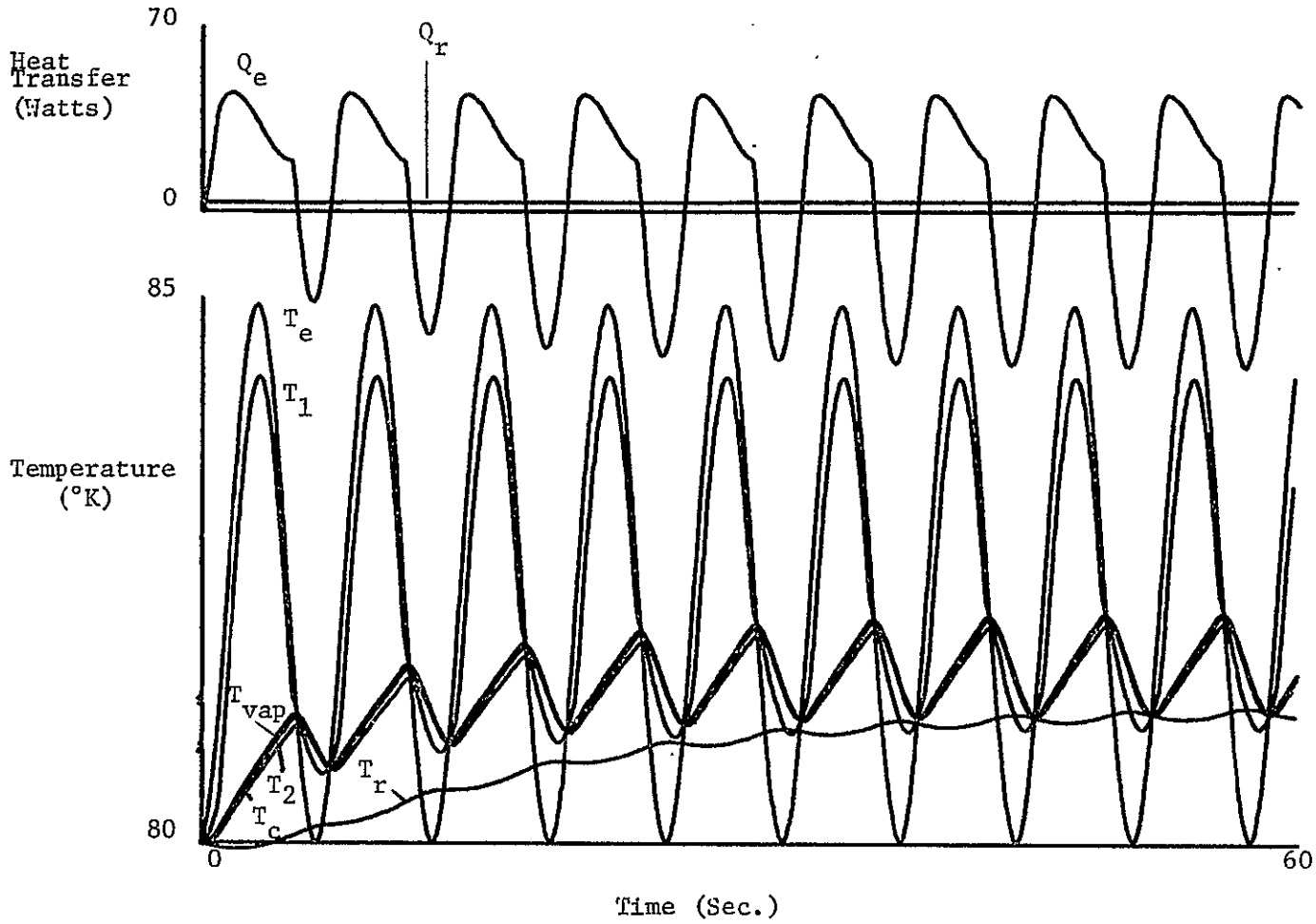

Figure 26. Fast Sine Wave

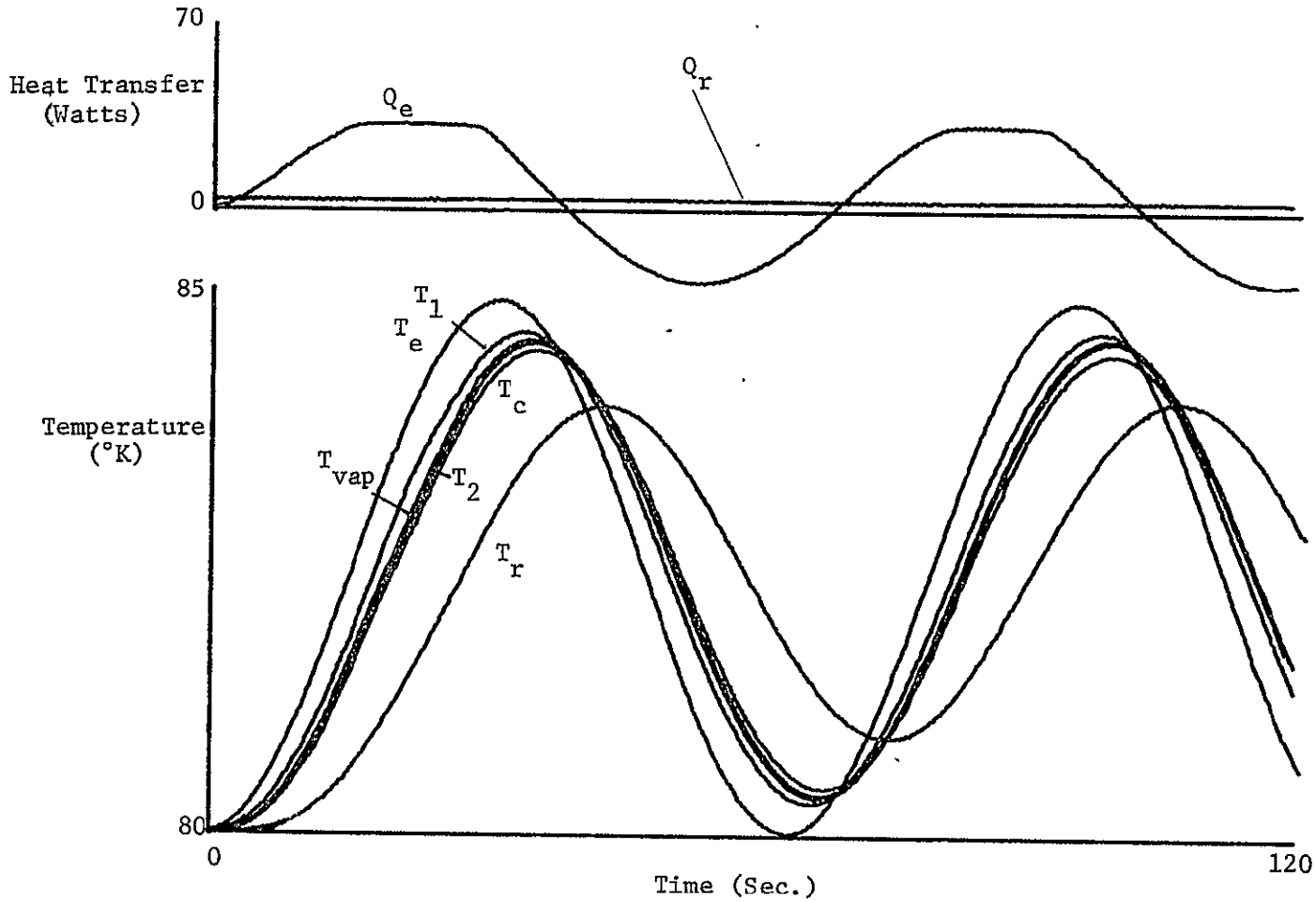

Figure 27. Slow Sine Wave

new approach will allow predictions to be made for various start-up situations including start-up from the supercritical state.

The digital work is now in the early stages of development. Fluid dynamic affects have not yet been incorporated. However, it is anticipated that these important affects can be readily included at the appropriate stage.

In the preliminary model now being studied several assumptions are made. (See Figure 28)

Evaporator sadle:	lumped mass, contact resistance to pipe wall, known heat input or fixed temperature.
Wall:	nodes in r and θ directions, contact resistance to wick.
Wick:	dryout circumferentially as f(Q) innermost layer of nodes at same temperature as vapor.
Vapor:	lumped system, includes mass of slab, linear temperature drop along tube.
Adiabatic section and condenser:	nodes in r,z directions, nodes become active as f(Q), innermost node of wick at same temperature as vapor.
Wick:	contact resistance to pipe wall.
Wall:	contact resistance to radiator.
Radiator:	lumped mass with known heat input or fixed temperature.
Axial conduction:	evaporator temperatures averaged for boundary condition in adiabatic section, weighted fraction of total heat transfer in axial direction subtracted from each evaporator node.

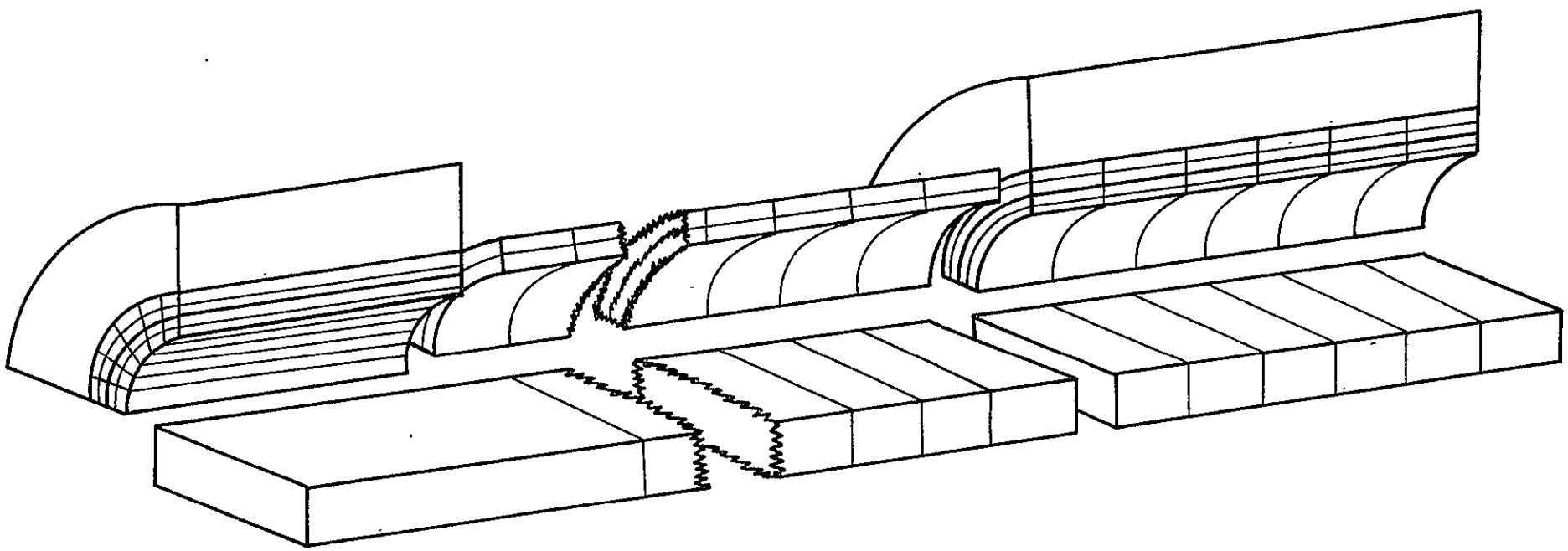

Figure 28. Heat Pipe Model

Thermal properties: constant at the temperature of the last time step.

The nomenclature used in the digital approach is:

A_R area of radiator

c_R specific heat of radiator

c_s specific heat of saddle

c_v specific heat of vapor and slab

k_w thermal conductivity of wick

ℓ_c length of adiabatic and condenser section

ℓ_e length of evaporator

m_R mass of radiator

m_s mass of saddle

m_v mass of vapor and slab

NIE number radial nodes in evaporator

NJE number circumferential nodes in evaporator

NIC number radial nodes in condenser

NJC number axial nodes in condenser

Q_{IR} heat input to radiator from space

Q_{Is} heat input to saddle

R_c contact resistance pipe to saddle or radiator

r_I inside radius of pipe

r_i radius at node i

r_o outside radius of pipe

$T_{c_{i,j}}^{n}$ temperature of condenser node i,j at time step n

$T_{E_{i,j}}^{n}$ evaporator node temperature at i,j

T_R radiator temperature

T_s saddle temperature

T_v vapor temperature

α thermal diffusivity of pipe wall

Δx $1/NI \ln(r_o/r_I)$ (see coordinate transformation)

Δy $2\pi/NJE$ (circumferential node width)

Δz ℓ_c/NJC (axial node width)

$\Delta\theta$ time increment

ε emissivity of radiator

σ Stefan-Boltzman constant

It is convenient to transform from cylindrical to rectangular coordinates.

In cylindrical coordinates $\bar{\nabla}^2 T$ is

$$\frac{\partial^2 T}{\partial r^2} + \frac{1}{r}\frac{\partial T}{\partial r} + \frac{1}{r}\frac{\partial^2 T}{\partial \phi^2} + \frac{\partial^2 T}{\partial z^2}$$

Make the following substitutions (See Figure 29).

$$x = \ln r/r_c$$

$$y = \phi$$

$$z = z$$

thus

$$\frac{\partial T}{\partial r} = \frac{\partial T}{\partial x}\frac{dx}{dr} + \frac{\partial T}{\partial \phi}\frac{dy}{dr} = \frac{1}{r}\frac{\partial T}{\partial x}$$

$$\frac{\partial^2 T}{\partial r^2} = \frac{\partial}{\partial r}\left(\frac{1}{r}\frac{\partial T}{\partial x}\right) = \frac{\partial^2 T}{\partial x^2}\frac{1}{r^2} - \frac{1}{r^2}\frac{\partial T}{\partial x}$$

$$\frac{\partial^2 T}{\partial \phi^2} = \frac{\partial^2 T}{\partial y^2}$$

$$\frac{\partial^2 T}{\partial z^2} = \frac{\partial^2 T}{\partial z^2}$$

Substitution into $\bar{\nabla}^2 T$

$$\frac{1}{r^2}\frac{\partial^2 T}{\partial x^2} - \frac{1}{r^2}\frac{\partial T}{\partial x} + \frac{1}{r^2}\frac{\partial T}{\partial x} + \frac{1}{r^2}\frac{\partial T}{\partial y^2} + \frac{\partial^2 z}{\partial z^2}$$

or

$$\frac{1}{r^2}\frac{\partial^2 T}{\partial x^2} + \frac{1}{r^2}\frac{\partial^2 T}{\partial y^2} + \frac{\partial^2 T}{\partial z}$$

Figure 30 shows the transformed computer grid for each of the various regions. The computational procedure for each time step $\Delta\theta(n \rightarrow n+1)$ is: 1) Explicit Balance on T_s

$$T_s^{n+1} = \frac{Q_{IE}\,\Delta\theta}{m_s c_s} + \frac{2\Delta\theta\pi\, r_o\, \ell_e}{(NJE)(m_s)(c_s)(R_c)} \sum_{j=1}^{NJE} (T_{E_{i,j}}^{n} - T_s^{n}) + T_s^{n} ,$$

2) Explicit Balance on Vapor

$$T_v^{n+1} = \frac{2\Delta\theta\, k_w\, \ell_e\, \pi}{\Delta x\, m_v c_v\, NJE} \sum_{j=1}^{NJE} (T_{E_{NJE-1,j}}^{n} - T_v^{n})$$

$$+ \frac{2\Delta\theta\, k_w\, \ell_c\, \pi}{\Delta x\, m_v c_v\, NJC} \sum_{j=1}^{NJC} (T_{c_{NJC-1,j}}^{n} - T_v^{n}) + T_v^{n} ;$$

3) Explicit Balance on Radiator

$$T_R^{n+1} = \frac{2\Delta\theta\, \ell_c\, \pi\, r_o}{m_R c_R\, R_c\, NJC} \sum_{j=1}^{NJC} (T_{c_{i,j}}^{n} - T_R^{n})$$

$$- \frac{A_R\, \sigma\, \epsilon\, \Delta\theta}{m_R c_R} (T_R^{4}) + \frac{Q_{IR}\,\Delta\theta}{m_R c_R} + T_R^{n} ;$$

4) Alternating direction implicit evaluation of evaporator grid. (developed next page); and

5) Alternating direction implicit evaluation of condenser grid. (similar to 4)

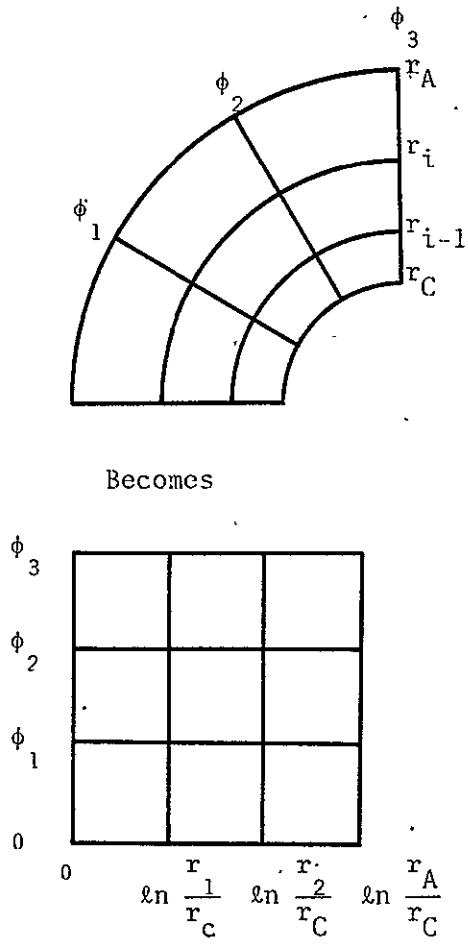

Figure 29. Polar to Rectangular Transformation

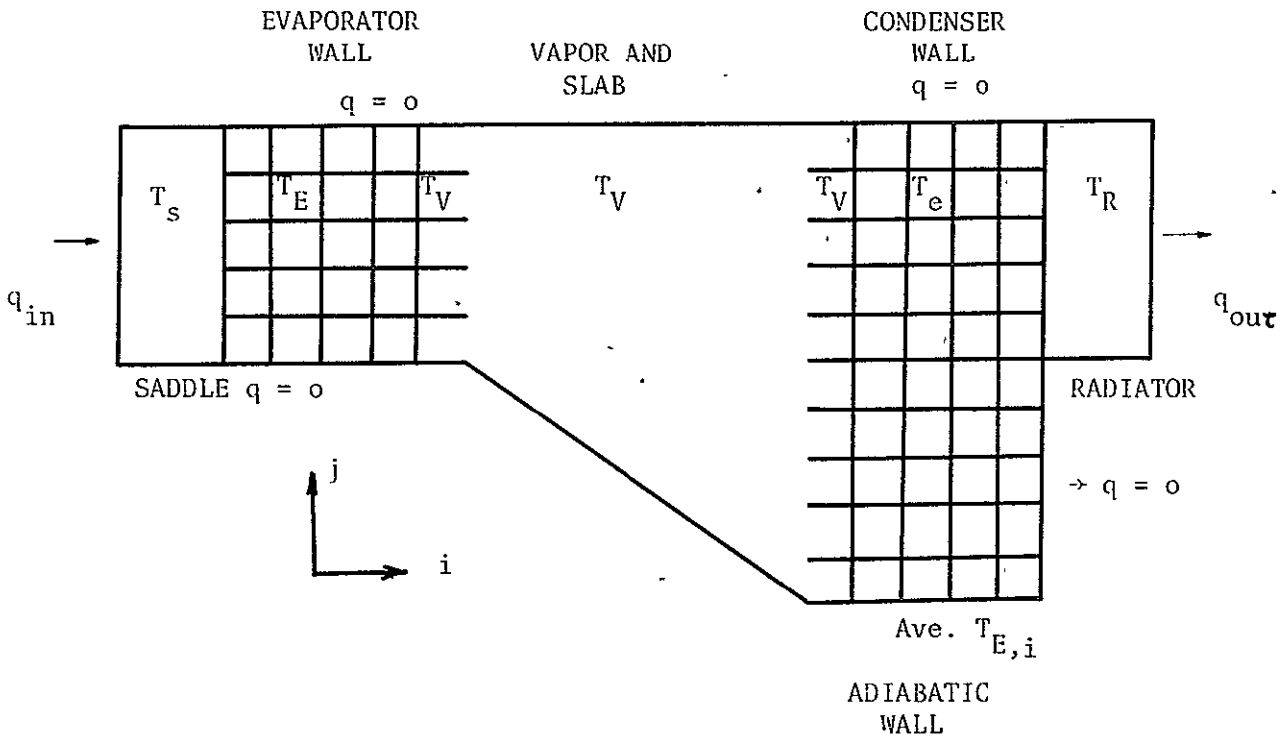

Figure 30. Computation Grid

As an example of the implicit equations used, consider an interior evaporator node for an i sweep.

$$\frac{r_i^2}{\alpha}\,\frac{T_{E_{i,j}}^{n+1/2} - T_{E_{i,j}}^{n}}{\Delta\theta/2} = \frac{1}{(\Delta x)^2}\left(T_{E_{i-1,j}}^{n+1/2} + T_{E_{i+1,j}}^{n+1/2} - 2T_{E_{i,j}}^{n+1/2}\right) + \frac{1}{(\Delta y)^2}\left(T_{E_{i,j-1}}^{n} + T_{E_{i,j+1}}^{n} - 2T_{E_{i,j}}^{n}\right)$$

$$-\left(\frac{T_{E_{i,j}}^{n}}{\sum_{j-1}^{NJE} T_{E_{i,j}}^{n}}\right)\left(T_{c_{i,1}}^{n} - \frac{1}{NJE}\sum_{j=1}^{NJE} T_{E_{i,j}}^{n}\right)\left(\frac{r_i}{\Delta z}\right)^2$$

The equation can be rewritten as

$$-\left(\frac{\Delta\theta}{2(\Delta x)^2}\right)\left(T_{E_{i-1,j}}^{n+1/2}\right) + \left(\frac{r_i^2}{\alpha} + \frac{\Delta\theta}{(\Delta x)^2}\right)\left(T_{E_{i,j}}^{n+1/2}\right) - \left(\frac{\Delta\theta}{2(\Delta x)^2}\right)\left(T_{E_{i,j+1}}^{n+1/2}\right) =$$

$$\frac{\Delta\theta}{2(\Delta y)^2}\left(T_{E_{i,j+1}}^{n} + T_{E_{i,j-1}}^{n}\right) + \left(\frac{r_i^2}{\alpha} - \frac{\Delta\theta}{(\Delta y)^2}\right) T_{E_{i,j}}^{n}$$

$$-\left(\frac{r_i^2\,\Delta\theta}{2(\Delta z)^2}\right)\left(\frac{T_{E_{i,j}}^{n}}{\sum_{j=1}^{NJE} T_{E_{i,j}}^{n}}\right)\left(T_{c_{i,1}}^{n} - \frac{1}{NJE}\sum_{j=1}^{NJE} T_{E_{i,j}}^{n}\right).$$

References 6 through 9 have been utilized extensively in developing the approach described above.

CONCLUSIONS

The primary general goal of this project was to develop techniques for predicting transient operation of cryogenic heat pipes. In particular the work was aimed towards development of schemes for predicting start up from various initial conditions such as those encountered in the supercritical regime. In accomplishing these goals it was necessary to first study steady state operation. The steady state work included prediction of performance limitations and thermal resistances. The transient part of the project has been divided into two areas: subcritical operation and supercritical operation.

During calendar 1975 the steady state part of the program was essentially completed and some results of computations are included in this report. The development of schemes for predicting transient operation is progressing well at this time and some preliminary results are included herein.

It is significant to note that several graduate and undergraduate students have received valuable training while performing tasks under this grant. One M.S. thesis, directly related to the project, was published during 1975 and it is expected that another one will be completed about July 1976.

REFERENCES

1. Hare, J. D., "Performance of a Nitrogen Heat Pipe with Various Capillary Structures", M.S. Thesis, Georgia Institute of Technology June 1975.

2. Williams, C. L., and G. T. Colwell, "Heat Pipe Model Accounting for Variable Evaporator and Condenser Lengths", AIAA Journal, Volume 12, Number 9, September 1974.

3. Abhat, A. and R. A. Seban, "Boiling and Evaporation From Heat Pipe Wicks with Water and Acetone", ASME Journal of Heat Transfer, Aug. 1974.

4. Levitan, M. M. and T. L. Perelman, "Fundamentals of Heat Pipe Theory and Design", Sov. Phys. Tech. Phys., Vol. 19, No. 8, February 1975.

5. Chun, K. R., "Some Experiments-on Screen Wick Dry-Out Limits", ASME Paper 71-WA/HT-6.

6. Roache, Patrick J., Computational Fluid Dynamics, Hermosa Publishers, Albuquerque, N.M., 1972.

7. Clausing, A. M., "Numerical Methods in Heat Transfer", Advanced Heat Transfer, Ed. by B. T. Chao, University of Illinois Press, Chicago, 1969.

8. Larkin, B. K., "Some Stable Explicit Approximations to the Diffusion Equation", Mathematics of Computation, 18, 196-202 (1964).

9. Carnahan, B., H. A. Luther, and J. O. Wilkes, Applied Numerical Methods, Wiley, New York, 1957.

DISTRIBUTION

1. (2 copies) NASA Scientific and Technical Information Facility, Post Office Box 33, College Park, Maryland 20740.

2. NASA Ames Research Center, Moffett Field, California 94035
   (5 copies) John P. Kirkpatrick
   Robert J. Debs
   Manfred Groll
   Craig McCreight
   Masahide Murakami
   Ray H. Sutton

3. NASA Goddard Space Flight Center, Code 732, Greenbelt, Maryland 20771
   (5 copies) Stanford Ollendorf
   Yashuhiro Kamotani
   Roy McIntosh
   Allan Sherman

4. John D. DiBattista, Mail Stop 158B, LDEF Project Office, NASA Langley Research Center, Hampton, Virginia 23665

5. Georgia Institute of Technology
   (5 copies) Office of Research Administration
   Vice President for Research
   Dean, College of Engineering
   (3 copies) Director, School of Mechanical Engineering
   (20 copies) Gene T. Colwell

APPENDIX

THERMAL RESISTANCE PROGRAM

```
      PROGRAM MAIN(INPUT,OUTPUT,TAPE5=INPUT,TAPE6=OUTPUT)
C
C
C     THERMAL ANALYSIS OF A CRYOGENIC HEAT PIPE
C
C               WRITTEN BY DAVID RUIS        10/29/75
C
C
C        UNITS OF INPUT QUANTITIES ARE AS FOLLOWS ---
C       TEMPERATURE R      Q ---BTU/HR    LENGTH ---FT
C
      DIMENSION AYTV(203),AYDT(203),AYQ(203),AYRTOT(203),AYRPE(203),
     CAYRWE(203),AYRTE(203),AYRV(203),AYRIC(203),AYRWC(203),AYRPC(203),
     CAYTC(203)
      DIMENSION IB(512)
      DIMENSION TV5(203),RT5(203),RPE5(203),RWE5(203),RTE5(203),RV5(203)
     C,RIC5(203),RWC5(203),RPC5(203)
      DIMENSION TV1(203),TV11(203),RT1(203),RT11(203),RWE1(203),
     CRWE11(203),RWC1(203),RWC11(203)
      REAL N,KW,KF,KL
      REAL LCA,LE,MUV,LFFF,LCD,LASTT
      INTEGER COUNT,CT
      INTEGER SYM
      KW(TZV)=KL(TZV)/((DF/(2.0*RF))*(2.0*(KL(TZV)/KF(TZV))+DF/(2.0*RF)
     C-2.0))+2.0*KL(TZV)/((DF/(2.0*RF))*((KL(TZV)/KF(TZV))*((2.0*RF)/
     C(DF-2.0*RF)+1.0)))+KL(TZV)/(2.0*RF/(DF-2.0*RF)+1.0)**2.0
      KF(TYV)=-4.02016E-5*TYV**2.0+3.20878E-2*TYV+1.30266
      FUNCB(DTV,DTAV)=(DTV-TPCI)/((QMAX/(2.0*PI*KW(DTAV)*LCD))*SUMA
     C+(QMAX/(2.0*PI*KL(DTAV)*LCD))*SUMB)-1.0
      KL(TXV)=1.0970566E-11*TXV**5.0-9.2427627E-9*TXV**4.0
     C+3.090593E-6*TXV**3.0-5.1457532E-4*TXV**2.0+4.2210737E-2*TXV
     C-1.26105
      FUNCC(DTPEI,D2TAV)=((DTPEI-TV)/((PI/(2.0*THETA))*((1.0/(2.0*PI
     C*KW(D2TAV)*LE))*SUMA+(1.0/(2.0*PI*KL(D2TAV)*LE))*SUMB)))-Q
      FUNCA(T1)=(A1/4.0)*T1**3.0+(A1*TC/2.0+A2/2.0-A1*TC/4.0)*T1**
     C2.0+(A1*TC*TC/4.0+A2*TC/2.0+A3-A1*TC*TC/2.0-A2*TC/2.0)*T1-A1*TC
     C**3.0/4.0-A2*TC*TC/2.0-A3*TC-(QMAX/(2.0*PI*LCD))*ALOG(RA/RB)
      FUNCD(DTE)=(A1/4.0)*DTE**3.0+((-A1/4.0)*TPEI+(A1/2.0)*TPEI+A2/2.0)
     C*DTE*DTE+((-A1/2.0)*TPEI*TPEI-(A2/2.0)*TPEI+(A1/4.0)*TPEI*TPEI
     C+(A2/2.0)*TPEI+A3)*DTE+((-A1/4.0)*TPEI**3.0-(A2/2.0)*TPEI*TPEI
     C-A3*TPEI-Q*ALOG(RA/RB)/(4.0*THETA*LE))
      CALL PLOTS(IB,512,9,00)
      CALL PLOTMX(348.0)
      CALL PLOT(3.0,2.0,-3)
      XP=12.0
      DO 400 L=6,6
      GATE=0.0
      SYM=0
      WRITE(6,3333)
      READ(5,7111)WT,RF,DF,N,BETA
7111  FORMAT(T7,F12.8,T19,F12.8,T31,F12.8,T43,F5.1,T48,F12.8)
      WRITE(6,7222)L
7222  FORMAT(T70,"CASE #",T77,I2)
      WRITE(6,7777)
      WRITE(6,7229)
7229  FORMAT(T35,"WT",T50,"RF",T65,"DF",T77,"N",T87,"BETA")
      WRITE(6,7230)WT,RF,DF,N,BETA
```

```
7230  FORMAT(T30,F12.8,T45,F12.8,T60,F12.8,T75,F5.1,T82,F12.8)
      WRITE(6,7777)
      SLABTH=8.0E-3
      LE=0.5
      LCD=1.0
      RA=0.04167
      Q=102.39
      QMAX=102.39
      DQ=-6.826
      PI=3.14159
      A1=-4.02016E-5
      A2=3.20878E-2
      A3=1.30266
      TCINC=0.5879396985
      RR=RA-WT
      RC=RR-4.0*RF*N-BETA*(N-1.0)
      RCHD=(PI*RC*RC-2.0*RC*SLABTH)/(2.0*PI*RC-2.0*SLABTH+4.0*RC)
      DO 300 K=1,2
      TC=108.0
      DO 190 J=1,200
1     THETA=(PI/2.0)/(1.0+(Q/QMAX))
      NI=INT(N)
C
C           COMPUTING TPCI AND RPC
C
      COUNT=0
      EPS1=0.001
      TPCI=TC
      LASTT=TC
4     F=FUNCA(TPCI)
      IF(F)5,20,7
5     F1=F
      TP1=TPCI
6     TPCI=TPCI+0.5
      F=FUNCA(TPCI)
      IF(F)6,20,10
7     F2=F
      TP2=TPCI
8     TPCI=TPCI+0.5
      F=FUNCA(TPCI)
      IF(F)9,20,8
9     F1=F
      TP1=TPCI
      GO TO 13
10    F2=F
      TP2=TPCI
      GO TO 13
13    TP3=(TP1*F2-TP2*F1)/(F2-F1)
      F3=FUNCA(TP3)
      ZA=ABS(LASTT-TP3)
      LASTT=TP3
      IF(ZA-EPS1)21,21,14
14    TP1=TP2
      TP2=TP3
      F1=F2
      F2=F3
      COUNT=COUNT+1
```

```
      GO TO 13
20    WRITE(6,1030)TPCI
1030  FORMAT(T30,"TPCI =",T38,F7.2,T50,"DOUBTFUL")
      GO TO 30
21    TPCI=TP3
      IF(GATE.NE.0.0)GO TO 30
      WRITE(6,1040)TPCI,COUNT,F3
1040  FORMAT(T30,"TPCI =",T38,F7.2,T50,"COUNT =",T59,I5,T65,"F =",T69,
     CF6.3)
      WRITE(6,2222)
30    TAV=(TPCI+TC)/2.0
      RPC=ALOG(RA/RB)/(2.0*PI*(A1*TAV*TAV+A2*TAV+A3)*LCD*(Q/QMAX))
C
C       COMPUTING TV AND RWC
C
      PSUM=0.0
      DO 40I=1,NI
      FI=FLOAT(I)
      TERM=ALOG((RB-(FI-1.0)*4.0*RF-(FI-1.0)*BETA)/(RB-4.0*FI*RF-(FI-1)
     C*BETA))
      PSUM=TERM+PSUM
40    CONTINUE
      SUMA=PSUM
      PSUM=0.0
      NM1=NI-1
      DO 42I=1,NM1
      FI=FLOAT(I)
      TERM=ALOG((RB-4.0*FI*RF-(FI-1.0)*BETA)/(RB-4.0*FI*RF-FI*BETA))
      PSUM=TERM+PSUM
42    CONTINUE
      SUMB=PSUM
      IF(NM1.EQ.0)SUMB=0.0
C
C   ITERATIVE SOLUTION BY LINEAR INTERPOLATION METHOD
C
50    TV=TPCI
      EPS2=0.001
51    TAV=(TV+TPCI)/2.0
52    F=FUNCB(TV,TAV)
      IF(F)60,90,70
60    F1=F
      TVX1=TV
61    TV=TV+5.0
      TAV=(TV+TPCI)/2.0
      F=FUNCB(TV,TAV)
      IF(F)61,90,63
63    F2=F
      TV2=TV
      GO TO 79
68    F2=F
      TV2=TV
70    TV=TV+5.0
      TAV=(TV+TPCI)/2.0
      F=FUNCB(TV,TAV)
      IF(F)71,90,70
71    F1=F
      TVX1=TV
```

```
      COUNT=0
      TV3=(TVX1*F2-TV2*F1)/(F2-F1)
      TAV=(TV3+TPCI)/2.0
      COUNT=COUNT+1
      ZB=ABS(TV3-TV2)
      IF(ZB.LE.EPS2)GO TO 91
      F3=FUNCB(TV3,TAV)
      F1=F2
      TVX1=TV2
      F2=F3
      TV2=TV3
      GO TO 80
90    WRITE(6,2010)TV,COUNT
2010  FORMAT(T50,"TV =",T55,F8.2,T65,"COUNT =",T73,I5,T85,"DOUBTFUL")
91    TV=TV3
      IF(GATE.NE.0.0)GO TO 95
      WRITE(6,2000)TV,COUNT,F3
2000  FORMAT(T30,"TV =",T35,F8.2,T50,"COUNT =",T58,I5,T65,"F =",T69,
     CF6.3)
      WRITE(6,2222)
95    CONTINUE
      RWC=(1.0/(2.0*PI*KW(TAV)*LCD*Q/QMAX))*SUMA+(1.0/(2.0*PI*KL(TAV)*LC
     CD*Q/QMAX))*SUMB
C
C     AT EVAPORATOR --- COMPUTATION OF TPEI AND RWE
C
      TPEI=TV
      TAV=(TPEI+TV)/2.0
      F=FUNCC(TPEI,TAV)
      IF(F)100,125,115
100   TP1=TPEI
      F1=F
102   TPEI=TPEI+5.0
      TAV=(TPEI+TV)/2.0
      F=FUNCC(TPEI,TAV)
      IF(F)102,125,105
105   TP2=TPEI
      F2=F
      GO TO 120
115   TP2=TPEI
      F2=F
116   TPEI=TPEI+5.0
      TAV=(TPEI+TV)/2.0
      F=FUNCC(TPEI,TAV)
      IF(F)116,125,119
119   TP1=TPEI
      F1=F
120   COUNT=0
      EPS3=0.001
121   TP3=(TP1*F2-TP2*F1)/(F2-F1)
      COUNT=COUNT+1
      TAV=(TP3+TV)/2.0
      ZC=ABS(TP3-TP2)
      IF(ZC.LE.EPS3)GO TO 124
      F3=FUNCC(TP3,TAV)
      F1=F2
      TP1=TP2
```

```
      F2=F3
      TP2=TP3
      GO TO 121
125   WRITE(6,2080)TPEI,COUNT
2080  FORMAT(T50,"TPEI =",T57,F8.2,T67,"COUNT =",T75,I5,T85,"DOUBTFUL").
124   IF(GATE.NE.0.0)GO TO 130
126   WRITE(6,2090)TP3,COUNT,F3
2090  FORMAT(T30,"TPEI =",T37,F8.2,T50,"COUNT =",T58,I5,T64,"F =",T68,
     CF6.3)
      WRITE(6,2222)
130   TPEI=TP3
      RWE=(PI/(2.0*THETA))*((1.0/(2.0*PI*LE))*(SUMA/KW(TAV)+SUMB/KL(TAV
     C)))
C
C     COMPUTATION OF TF AND RPE
C
      TE=TPEI
      F=FUNCD(TE)
      IF(F)150,180,165
150   TE1=TE
      F1=F
151   TE=TE+1.0
      F=FUNCD(TE)
      IF(F)151,181,153
153   TE2=TE
      F2=F
      GO TO 170
165   TE2=TE
      F2=F
166   TE=TE+1.0
      F=FUNCD(TE)
      IF(F)168,181,166
168   TE1=TE
      F1=F
170   CT=0
      EPS4=0.001
171   TE3=(TE1*F2-TE2*F1)/(F2-F1)
      CT=CT+1
      ZD=ABS(TE3-TE2)
      IF(ZD.LE.EPS4)GO TO 180
      F3=FUNCD(TE3)
      F1=F2
      TE1=TE2
      F2=F3
      TE2=TE3
      GO TO 171
180   TE=TE3
      F=F3
      IF(GATE.NE.0.0)GO TO 183
181   WRITE(6,3030)TE,F,CT
3030  FORMAT(T30,"TE =",F8.2,T45,"F =",T46,F10.3,T60,"CT =",I65,I5)
183   TAV=(TF+TPEI)/2.0
      RPE=(PI/(2.0*THETA))*ALOG(RA/RB)/(2.0*PI*LE*KF(TAV))
C
C     COMPUTATION OF INTERFACIAL RESISTANCE
C
      HFG=778.16*(-4.11334E-11*TV**6.0+2.0908E-8*TV**5.0-1.43119E-6*
```

```
      CTV**4.0-1.03235E-3*TV**3.0+2.61594E-1*TV*TV-2.40246E+1*TV+8.89614
      CE+2)
       PV=1.71041E-6*TV**5.0-1.20901E-3*TV**4.0+3.71275E-1*TV**3.0
      C-5.70868E+1*TV*TV+4.28513E+3*TV-1.25125E+5
       LCA=LCD*Q/QMAX
C
C     UNITS OF RIC AS COMPUTED HERE ARE (SEC R / LBF FT)
C
       RIC=14.408*TV**2.5/(RC*LCA*PV*HFG*HFG)
       RIE=(PI/(2.0*THETA))*RIC*LCA/LE
C
C      COMPUTATION OF VAPOR RESISTANCE
C         UNITS ARE (SEC R / LBF FT )
C
       LEFF=3.0-LE/2.0-LCD*Q/(2.0*QMAX)
       MUV=8.5591E-21*TV**7.0-6.55918E-18*TV**6.0+1.70105E-15*TV**5.0-8.
      C08533E-14*TV**4.0-4.27309E-11*TV**3.0+8.90377E-9*TV*TV-6.94007E-7
      C*TV+1.99577E-5
       ROV=1.39324E-13*TV**7.0-1.042325E-10*TV**6.0+2.638736E-8*TV**5.0
      C-1.14015E-6*TV**4.0-6.78395E-4*TV**3.0+1.385489E-1*TV*TV-1.07628
      CE+1*TV+3.10045E+2
       ROL=-5.8917E-13*TV**7.0+4.50297E-10*TV**6.0-1.15298E-7*TV**5.0+4.9
      C5327E-6*TV**4.0+2.9749E-3*TV**3.0-5.98552E-1*TV*TV+4.54425E+1*TV-1
      C.21455E+3
       RV=8.0*MUV*LEFF*TV*(1.0/ROV-1.0/ROL)/(PI*ROV*HFG*HFG*RCHD**4.0)
C
C            UNIT CONVERSION
C
       S1=0.4097
       RVSI=S1*RV
       RIESI=S1*RIE
       RICSI=S1*RIC
       S2=1.8957
       RPCSI=S2*RPC
       RPESI=S2*RPE
       RWCSI=S2*RWC
       RWESI=S2*RWE
       S3=0.5556
       TCSI=S3*TC
       TPCTSI=S3*TPCI
       TVSI=S3*TV
       TPETSI=S3*TPEI
       TESI=S3*TE
       QSI=Q*0.2930
       RTOT=RPESI+RWESI+RIESI+RVSI+RICSI+RWCSI+RPCSI
       S4=304.8
       XRTOT=(TESI-TCSI)/QSI
       DFSI=S4*DF
       RFSI=S4*RF
       BETASI=S4*BETA
       RASI=S4*RA
       WISI=S4*WI
       DELTAT=TESI-TCSI
C
C       WRITING AND SETTING UP ARRAYS
C
       IF(K.NE.1)GO TO 185
```

```
      TV1(J)=TVSI
      RT1(J)=RTOT
      RWE1(J)=RWESI
      RWC1(J)=RWCSI
      GO TO 188
  185 IF(K.NE.11)GO TO 187
      TV11(J)=TVSI
      RT11(J)=RTOT
      RWE11(J)=RWESI
      RWC11(J)=RWCSI
      GO TO 188
  187 IF(K.NE.5)GO TO 188
      TV5(J)=TVSI
      RT5(J)=RTOT
      RPE5(J)=RPESI
      RWE5(J)=RWESI
      RIE5(J)=RIESI
      RV5(J)=RVSI
      RIC5(J)=RICSI
      RWC5(J)=RWCSI
      RPC5(J)=RPCSI
  188 CONTINUE
      AYTV(J)=TVSI
      AYDT(J)=DELTAT
      AYQ(J)=QSI
      AYRTOT(J)=RTOT
      AYRPE(J)=RPESI
      AYRWE(J)=RWESI
      AYRIE(J)=RIESI
      AYRV(J)=RVSI
      AYRIC(J)=RICSI
      AYRWC(J)=RWCSI
      AYRPC(J)=RPCSI
      AYIC(J)=TCSI
      GAIE=1.0
      TC=TC+TCINC
  190 CONTINUE
      WRITE(6,3333)
 3333 FORMAT(1H1)
      WRITE(6,6063)
 6063 FORMAT(T20,"UNITS ---",T55,"TEMPERATURE -- K",T55,"RESISTANCE -- K
     C/WATT",T79,"HEAT TRANSFER RATE -- WATTS")
      WRITE(6,7777)
      WRITE(6,7777)
      WRITE(6,7777)
      WRITE(6,7777)
 7777 FORMAT(1H0)
      WRITE(6,5005)
 5005 FORMAT(T5,"Q",T22,"TV",T29,"DELTAT",T38,"RTOT",T49,"RPE",T60,
     C"RWE",T71,"RIE",T82,"RV",T93,"RIC",T104,"RWC",T115,"RPC",T126,"TC"
     C)
      WRITE(6,2222)
      DO 200 J=1,200,6
      WRITE(6,5000)AYQ(J),AYTV(J),AYDT(J),AYRTOT(J),AYRPE(J),AYRWE(J),AY
     CRIE(J),AYRV(J),AYRIC(J),AYRWC(J),AYRPC(J),AYIC(J)
 5000 FORMAT(T2,F6.2,T20,F6.2,T28,F6.2,T35,E10.4,T46,E10.4,T57,E10.4,
     CT68,E10.4,T79,E10.4,T90,E10.4,T101,E10.4,T112,E10.4,T123,F8.2)
```

```
  200   CONTINUE
        Q=Q+DQ
C
C          PLOTTING DT .VS. TV AT CONSTANT Q
C
        IF(K.NE.1)GO TO 510
        CALL SCALE(AYTV,6.0,200,+1)
        FVTV=AYTV(201)
        DVTV=AYTV(202)
        AYDT(201)=0.0
        CALL SCALE(AYDT,7.0,201,+1)
        FVDT=AYDT(202)
        DVDT=AYDT(203)
        CALL AXIS(0.0,0.0,17HVAPOR TEMPERATURE,-17,6.0,0.0,FVTV,DVTV)
        CALL AXIS(0.0,0.0,7HDELTA T,+7,7.0,90.0,FVDT,DVDT)
  510   CONTINUE
        AYTV(201)=FVTV
        AYTV(202)=DVTV
        AYDT(201)=FVDT
        AYDT(202)=DVDT
        CALL LINE(AYTV,AYDT,200,1,+50,SYM)
        SYM=SYM+1
  300   CONTINUE
        CALL PLOT(XP,0.0,-3)
C                 ARRAY #5
C          PLOTTING RTOT,RWE,RWC, VS.  TV
C
        CALL SCALE(TV5,6.0,200,+1)
        FVTV=TV5(201)
        DVTV=TV5(202)
        RT5(201)=0.0
        CALL SCALE(RT5,7.0,201,1)
        FVR=RT5(202)
        DVR=RT5(203)
        RT5(201)=FVR
        RT5(202)=DVR
        CALL AXIS(0.0,0.0,17HVAPOR TEMPERATURE,-17,6.0,0.0,FVTV,DVTV)
        CALL AXIS(0.0,0.0,18HTHERMAL RESISTANCE,+18,7.0,90.0,FVR,DVR)
        SYM=1
        CALL LINE(TV5,RT5,200,1,+50,SYM)
        SYM=SYM+1
        RWE5(201)=FVR
        RWE5(202)=DVR
        RWC5(201)=FVR
        RWC5(202)=DVR
        CALL LINE(TV5,RWE5,200,1,+50,SYM)
        SYM=SYM+1
        CALL LINE(TV5,RWC5,200,1,+50,SYM)
C
C            PLOTTING RPE,RPC, VS. TV
C
        SYM=SYM+1
        CALL PLOT(XP,0.0,-3)
        IF(RPE5(1).GT.RPC5(1))610,615
  610   RPE5(201)=0.0
        CALL SCALE(RPE5,7.0,201,1)
        FVR=RPE5(202)
```

```
      DVR=RPE5(203)
      GO TO 618
615   RPC5(201)=0.0
      CALL SCALE(RPC5,7.0,201,1)
      FVR=RPC5(202)
      DVR=RPC5(203)
618   CONTINUE
      RPE5(201)=FVR
      RPE5(202)=DVR
      RPC5(201)=FVR
      RPC5(202)=DVR
      CALL AXIS(0.0,0.0,17HVAPOR TEMPERATURE,-17,6.0,0.0,FVTV,DVTV)
      CALL AXIS(0.0,0.0,18HTHERMAL RESISTANCE,+18,7.0,90.0,FVR,DVR)
      CALL LINE(IV5,RPE5,200,+1,+50,SYM)
      SYM=SYM+1
      CALL LINE(IV5,RPC5,200,+1,+50,SYM)
C
C        PLOTTING RIE,RIC VS. IV
C
      SYM=SYM+1
      CALL PLOT(XP,0.0,-3)
      IF(RIE5(1).GT.RIC5(1))650,655
650   RIE5(201)=0.0
      CALL SCALE(RIE5,7.0,201,1)
      FVR=RIE5(202)
      DVR=RIE5(203)
      GO TO 659
655   RIC5(201)=0.0
      CALL SCALE(RIC5,7.0,201,1)
      FVR=RIC5(202)
      DVR=RIC5(203)
659   CONTINUE
      RIE5(201)=FVR
      RIE5(202)=DVR
      RIC5(201)=FVR
      RIC5(202)=DVR
      CALL AXIS(0.0,0.0,17HVAPOR TEMPERATURE,-17,6.0,0.0,FVTV,DVTV)
      CALL AXIS(0.0,0.0,18HTHERMAL RESISTANCE,+18,7.0,90.0,FVR,DVR)
      CALL LINE(IV5,RIE5,200,1,+50,SYM)
      SYM=SYM+1
      CALL LINE(IV5,RIC5,200,1,+50,SYM)
C
C         PLOTTING RV VS. IV
C
      SYM=SYM+1
      CALL PLOT(XP,0.0,-3)
      CALL SCALE(RV5,7.0,200,+1)
      FVR=RV5(201)
      DVR=RV5(202)
      CALL AXIS(0.0,0.0,17HVAPOR TEMPERATURE,-17,6.0,0.0,FVTV,DVTV)
      CALL AXIS(0.0,0.0,18HTHERMAL RESISTANCE,+18,7.0,90.0,FVR,DVR)
      CALL LINE(IV5,RV5,200,1,0,0)
C           ARRAYS = 1
C
C         RTOT,RWF,RWC
C
      SYM=SYM+1
```

```
      CALL PLOT(XP,0.0,-3)
      CALL SCALE(TV1,6.0,200,+1)
      FVTV=TV1(201)
      DVTV=TV1(202)
      RT1(201)=0.0
      CALL SCALE(RT1,7.0,201,1)
      FVR=RT1(202)
      DVR=RT1(203)
      RT1(201)=FVR
      RT1(202)=DVR
      RWE1(201)=FVR
      RWE1(202)=DVR
      RWC1(201)=FVR
      RWC1(202)=DVR
      CALL AXIS(0.0,0.0,17HVAPOR TEMPERATURE,-17,6.0,0.0,FVTV,DVTV)
      CALL AXIS(0.0,0.0,18HTHERMAL RESISTANCE,+18,7.0,90.0,FVR,DVR)
      CALL LINE(TV1,RT1,200,1,+50,SYM)
      SYM=SYM+1
      CALL LINE(TV1,RWE1,200,1,+50,SYM)
      SYM=SYM+1
      CALL LINE(TV1,RWC1,200,1,+50,SYM)
C
C           ARRAYS # 11
C
C           RT01,RWE,RWC
C
      SYM=SYM+1
      CALL PLOT(XP,0.0,-3)
      CALL SCALE(TV11,6.0,200,+1)
      FVTV=TV11(201)
      DVTV=TV11(202)
      RT11(201)=0.0
      CALL SCALE(RT11,7.0,201,1)
      FVR=RT11(202)
      DVR=RT11(203)
      RT11(201)=FVR
      RT11(202)=DVR
      RWE11(201)=FVR
      RWE11(202)=DVR
      RWC11(201)=FVR
      RWC11(202)=DVR
      CALL AXIS(0.0,0.0,18HTHERMAL RESISTANCE,+18,7.0,90.0,FVR,DVR)
      CALL AXIS(0.0,0.0,17HVAPOR TEMPERATURE,-17,6.0,0.0,FVTV,DVTV)
      CALL LINE(TV11,RT11,200,1,+50,SYM)
      SYM=SYM+1
      CALL LINE(TV11,RWE11,200,1,+50,SYM)
      SYM=SYM+1
      CALL LINE(TV11,RWC11,200,1,+50,SYM)
      CALL PLOT(XP,0.0,-3)
400   CONTINUE
      CALL PLOT(1.0,1.0,999)
2222  FORMAT(1H )
99    STOP
      END
```